Adiponectin pathway activation dampens inflammation and enhances alveolar macrophage fungal killing via LC3-associated phagocytosis

Sri Harshini Goli,[1,2*] Joo-Yeon Lim,[1*] Nese Basaran-Akgul,[1] and Steven P. Templeton[1,†]

[1] Department of Microbiology and Immunology, Indiana University School of Medicine-Terre Haute, Terre Haute, IN 47809, USA

[2] Department of Biology, Indiana State University, Terre Haute, IN 47809, USA

[*] These authors contributed equally to this work.

Short title: Adiponectin promotes LC3-mediated fungal killing by alveolar macrophages

[†]Correspondence: sptemple@iu.edu; Tel.:+1-821-237-8193

Abstract

Although innate immunity is critical for antifungal host defense against the human opportunistic fungal pathogen *Aspergillus fumigatus*, potentially damaging inflammation must be controlled. Adiponectin (APN) is an adipokine produced mainly in adipose tissue that exerts anti-inflammatory effects in adipose-distal tissues such as the lung. We observed 100% mortality and increased fungal burden and inflammation in neutropenic mice with invasive aspergillosis (IA) that lack APN or the APN receptors AdipoR1 or AdipoR2. Alveolar macrophages (AMs), early immune sentinels that detect and respond to lung infection, express both receptors, and APN-/- AMs exhibited an inflammatory/M1 phenotype that was associated with decreased fungal killing. Pharmacological stimulation of AMs with AdipoR agonist AdipoRon partially rescued deficient killing in APN-/- AMs that was dependent on both receptors. Finally, APN-enhanced fungal killing was associated with increased activation of the non-canonical LC3 pathway of autophagy. Thus, our study identifies a novel role for APN in LC3-mediated killing of *A.fumigatus*.

Author Summary

Aspergillus fumigatus is a human fungal pathogen that causes an often-fatal invasive infection of the lung in immune compromised individuals, a population that is increasing. Since current antifungal drugs have limited efficacy, it is important to identify pathways that may be pharmaceutically targeted to complement existing therapies. Adiponectin (APN) is an anti-inflammatory intercellular cytokine messenger produced mainly in adipose tissue that protects against invasive aspergillosis. Alveolar macrophages are early immune sentinel cells in the lung, and we report that AMs from mice lacking APN exhibit an inflammatory phenotype and reduced killing of *A. fumigatus* spores that is improved when AMs are treated with a drug (AdipoRon) that simulates APN binding to its receptors AdipoR1 and AdipoR2. Furthermore, APN was associated with activation of LC3-associated phagocytosis, a mechanism of fungal killing important for host defense against *A. fumigatus* infection. Thus, we identify therapeutic potential of the APN pathway in stimulation of immune-mediated fungal killing and treatment of fungal infection.

Keywords: invasive aspergillosis, *Aspergillus fumigatus*, adiponectin, adiponectin receptor, adipoRon, lung immune responses, alveolar macrophages, LC3-associated phagocytosis

54 **Introduction**

55 The human opportunistic fungal pathogen *Aspergillus fumigatus* is the primary etiologic agent of
56 invasive pulmonary aspergillosis (IA), a frequently severe infection with a high mortality rate [1].
57 Effective treatment options for IA remain limited, despite increases in the at-risk population, and fungal
58 resistance to existing antifungal drugs is increasing. Furthermore, although an underlying immune
59 deficiency renders individuals susceptible to IA, poor disease outcomes are associated with detrimental
60 inflammatory pathology [2,3]. It is thus critical to identify anti-inflammatory pathways that could be
61 exploited to target detrimental immune pathology, enhance antifungal immunity, and complement
62 existing antifungal therapies in IA patients.

63 Adiponectin (APN) is an anti-inflammatory adipokine produced mainly in adipose tissue and expressed
64 at high levels in lean and healthy individuals, whereas in obese individuals, adipose tissue is inflamed
65 and APN production and secretion are inhibited [4–6]. Numerous studies have demonstrated a
66 protective effect for APN in autoimmune and inflammatory diseases, and immune-mediated clearance
67 of *Listeria monocytogenes* was hampered in obese and APN-deficient mice due to detrimental
68 inflammation and hematopoietic dysfunction [7]. More recently, we demonstrated increased mortality,
69 fungal burden, lung inflammatory cytokine production and eosinophil recruitment in APN-deficient
70 mice with IA [8]. However, eosinophils did not play a significant role in the pathology of APN-
71 deficiency, as neutropenic mice deficient in both APN and eosinophils exhibited only delayed, but not
72 decreased mortality, suggesting other unidentified mechanisms of APN-mediated protection in IA.

73 Alveolar macrophages (AMs) are the primary immune sentinel of lung airways, and their early
74 responses to inhaled fungal conidia are critical for disease outcomes, particularly in
75 immunocompromised hosts [9,10]. In our previous study, we observed increased production of the pro-
76 inflammatory cytokine TNF in APN-/- AMs [8], suggesting that these cells contribute to the
77 inflammatory phenotype of APN-/- mice with IA. In this study, we aimed to determine how the
78 adiponectin pathway regulates responses of AMs to *A. fumigatus* infection. We report increased
79 production of inflammatory cytokines, an elevated M1 phenotype, and reduced uptake and killing of
80 conidia in APN-/- AMs that is increased by stimulation with the APN receptor agonist AdipoRon.
81 Furthermore, APN stimulation was associated with increased AM activation of the non-canonical
82 autophagy LC3 pathway in conidia-containing phagosomes, thus identifying a novel role for APN in

83 promoting LC3-associated phagocytosis (LAP) in antifungal immunity.

84 **Results**

85 **Increased mortality, fungal burden, and inflammatory pathology in APN pathway-deficient mice**
86 **with IA.**

87 Previously, we reported that APN inhibits inflammatory lung pathology during IA [8]. Since APN-/-
88 strains vary in their metabolic phenotypes[11–13], we confirmed the inflammatory phenotype of APN-
89 /- mice from a second strain (obtained from Dr. Philipp Scherer) (**Fig. S1**), and observed similar
90 increases in fungal burden (**Figs. S1B-S1D**), inflammatory cytokines and inflammatory cell recruitment
91 (**Figs. S1E-S1F** and **S1H**) while only survival and AdipoR1 transcription were not significantly
92 different from wild-type (WT) C57BL/6 controls (**Figs. S1A** and **S1G**, respectively). We also aimed to
93 determine the contribution of the canonical adiponectin receptors AdipoR1 and AdipoR2 to IA
94 pathology, and thus infected neutrophil-depleted WT, APN-/-, AdipoR1-/- and AdipoR2-/- mice to
95 compare mortality, pathology, fungal burden, inflammatory cell recruitment and cytokine production
96 (**Fig. 1A**). In contrast to WT mice, mortality was 100% in APN-/-, AdipoR1-/-, and AdipoR2-/- mice,
97 with mortality beginning on day 2 post-infection and 100% by day 6 p.i. (**Fig. 1B**), with extensive lung
98 hyphal growth and peri-bronchoalveolar inflammation (**Fig. 1C**) and increased fungal burden as
99 measured by qPCR of fungal DNA (**Fig. 1D**) and image quantification of fungal GMS staining (**Fig.**
100 **1E**). Inflammatory cells were increased in the bronchoalveolar lavage fluid (BALF), most significantly
101 in APN-/- mice (**Fig. 1F**), while lung inflammatory cytokines IL-1a, IL-6, TNF, IL-12b, and IL-17A
102 and the anti-inflammatory cytokine IL-10 were increased, most significantly in AdipoR1-/- mice (**Figs.**
103 **1G and 1H**). In summary, adiponectin-pathway deficiency is associated with increased mortality, lung
104 fungal burden, and inflammatory pathology, cell recruitment, and cytokine production. Furthermore,
105 disrupted signaling through either AdipoR1 or AdipoR2 results in increased IA severity.

106 **Alveolar macrophages (AMs) from adiponectin pathway-deficient mice exhibit an inflammatory**
107 **phenotype.**

108 Previously, we observed increased intracellular TNF in AMs from APN-/- mice with IA when
109 compared to WT AMs [8], and we observed mortality as early as day 2 post-infection in APN-
110 pathway-deficient mice with IA, suggesting a critical involvement of early immune effectors in
111 protection from infection. As AMs contribute to early responses to inhalation of *A. fumigatus* [9],

112 especially in immunocompromised hosts [10], we aimed to further examine the phenotype of AMs
113 from APN pathway-deficient hosts using primary ex vivo cultures. We observed expression of both
114 AdipoR1 and AdipoR2 in WT and APN-deficient mice that was decreased in lung tissue upon *A.*
115 *fumigatus* infection, but increased in the BALF (**Fig. S2A**), with the highest surface expression of
116 AdipoR1 in AMs (**Fig. S2B**). APN-pathway deficient AMs exhibited differential expression of
117 AdipoRs at the transcription level **Fig. S2C**), and infection of APN-/- AMs decreased AdipoR1
118 expression (**Fig. S2D**). Although WT, APN-/-, AdipoR1-/-, and AdipoR2-/- AMs were similar
119 morphologically (data not shown), transcription of IL-1α, IL-1β, IL-6, IL-17A, IL-23, and TNF was
120 increased in APN pathway-deficient AMs when compared WT-derived AMs, while IL-10 was similar
121 (**Fig. 2A**), and secreted TNF in the supernatant increased equally in response to infection in all groups
122 (**Fig. 2B**). To investigate the inflammatory phenotype more specifically in ex vivo cultured APN-/-
123 AMs, we compared expression of the macrophage polarization markers CD38 (M1/classical) and Egr2
124 (M2/alternative) with wild type WT AMs [14]. In a resting state, a higher percentage of APN-/- AMs
125 were CD38+ and lower percentage were Egr2+ when compared to WT (**Figs. 2C and 2D**), while upon
126 infection with *A. fumigatus*, percentages of both CD38+Egr2- and CD38-Egr2+ cells increased (**Figs.**
127 **2C and 2E**). These results suggest that APN pathway-deficient AMs exhibit an increased inflammatory
128 phenotype compared to WT AMs.

129 ***A. fumigatus* uptake and killing is inhibited in APN-/- AMs.**

130 Although APN pathway-deficient mice displayed increased IA severity, fungal burden, and an
131 increased AM inflammatory phenotype, the mechanism of decreased fungal clearance remains
132 unknown. To determine if APN-deficient AMs were deficient in fungal uptake and killing, we used
133 dual viability/tracking fluorescent *Aspergillus* reporter FLARE conidia [15]. to compare changes in
134 conidia uptake and viability in wild-type and APN-/- AMs ex vivo and in vivo. In APN-/- AMs
135 cultured ex vivo, uptake and killing of dual-labeled FLARE conidia was decreased after 6 hours when
136 observed by microscopy (**Fig. 3A** and **Supplemental Video SV1**). When loss of *A. fumigatus* viability
137 was compared by image analysis, killing of FLARE conidia by APN-/- AMs was markedly decreased
138 compared to wild-type AMs (**Fig. 3B**). Uptake and killing were also reduced in APN-/- AMs when
139 analyzed by flow cytometry, even after filtration to remove hyphae (**Figs 3C and 3D**). Reduced killing
140 by APN-/- AMs was confirmed in vivo in FLARE-infected neutropenic mice, with a significant
141 difference in conidial viability by day 3 post-infection (**Figs. 3E and 3F**), while uptake of 1 μm inert

142 particles was not significantly different between wild-type and APN-/- AMs (**Fig. 3G**). Collectively,
143 these results demonstrate that AM fungal uptake and killing are decreased in the absence of APN.

144 **The AdipoR agonist AdipoRon decreases inflammation and fungal burden in APN-deficient mice**
145 **with IA.**

146 A small molecule agonist (AdipoRon) that binds and activates signaling through both AdipoR1 and
147 AdipoR2 improved insulin resistance and glucose intolerance and increased the lifespan of obese mice
148 [16]. A role for AdipoRon in dampening inflammatory responses in human lung macrophages via
149 inhibition of production of TNF, IL-6, and inflammatory chemokine production has also been reported
150 [17]. However, the ability of AdipoRon therapy to improve IA outcomes remained unknown. We
151 treated infected neutropenic wild-type or APN-/- mice with AdipoRon by involuntary aspiration daily
152 for up to eight days (**Fig. 4A**). Although AdipoRon treatment did not significantly improve survival
153 (**Fig. 4B**), lung hyphal growth and fungal burden were reduced in APN-/- mice (**Figs. 4C-4E**). Airway
154 eosinophil recruitment was reduced in AdipoRon treated APN-/- mice, while AMs were increased in
155 both AdipoRon-treated WT and APN-/- mice (**Fig. 4F**). Transcription of IL-1a, IL-6, IL-10, IL-17A,
156 and TNF were also decreased with AdipoRon treatment in APN-/- lungs and decreases in IL-1a and IL-
157 10 were also evident in wild-type mice (**Fig. 4G**). In contrast, IL-12b transcription appeared to be
158 increased by AdipoRon, but only in wild-type lungs. An AdipoRon-mediated decrease in TNF was also
159 confirmed in APN-/- BALF at the protein level (**Fig. 4H**). These results indicate that APN pathway
160 stimulation by AdipoRon decreases lung fungal burden and dampens lung inflammation in APN-/-
161 mice with IA.

162 **AdipoRon increases fungal killing and inhibits the inflammatory phenotype of APN-/- AMs.**

163 Although AdipoRon treatment influenced lung fungal growth and dampened inflammation in APN-/-
164 mice with IA, the specific effect of AMs remained unknown. To determine the effect of AdipoRon on
165 AM phenotype and fungal uptake and killing, we infected WT or APN pathway-deficient AMs with
166 Af293 or FLARE conidia after 24 hours treatment with AdipoRon or control vehicle (containing
167 DMSO), and harvested AMs ten hours later for microscopic, flow cytometric, qRT-PCR, and ELISA
168 analyses (**Fig. 5A**). When quantified by microscopy, conidia viability was decreased by AdipoRon
169 treatment of APN-/- but not wild-type AMs (**Fig. 5B**). Conidia viability was also reduced in APN
170 pathway-deficient AMs by AdipoRon when measured by flow cytometry after cell straining to remove

171 hyphae (**Fig. 5C**). Inflammatory cytokine transcription of IL-1α, IL-1β, and IL-6 were all decreased by
172 AdipoRon treatment in APN-/- AMs, while the anti-inflammatory cytokine IL-10 was not affected by
173 AdipoRon regardless of APN sufficiency (**Fig. 5D**). Secretion of TNF protein was also significantly
174 decreased in AdipoRon-treated APN-/- AMs (**Fig. 5E**). These results indicate that AdipoRon treatment
175 acts on APN-/- AMs to improve fungal killing and inhibit an inflammatory phenotype.

176 **AdipoRon-enhanced killing of *A. fumigatus* requires both AdipoR1 and AdipoR2.**

177 Since AdipoRon enhances AM-mediated fungal killing, we aimed to confirm the requirement of
178 AdipoR1 and AdipoR2 by using siRNA to target expression of AdipoR1 in wild-type, APN-/-, and
179 AdipoR2-/- AMs (**Fig. 6A**). Decreased AM transcription of *Adipor1* and *Adipor2* by infection was
180 partially restored by AdipoRon treatment (**Fig. S2E**). Knockdown of AdipoR1 was confirmed by flow
181 cytometry to reduce expression to identical levels observed in AMs from AdipoR1-/- mice (**Figs. 6B**
182 **and 6C**). Moreover, fungal killing was improved by AdipoRon treatment in wild-type, APN-/-,
183 AdipoR1-/- (KO mice and siRNA), and AdipoR2-/- AMs, but was not improved with siRNA-targeted
184 depletion of AdipoR1 in AdipoR2-/- AMs (**Fig. 6D**). These results show that both canonical APN
185 receptors are critical for AdipoRon-mediated enhancement of AM fungal killing.

186 **Adiponectin promotes LC3-associated phagocytosis of *A. fumigatus* conidia.**

187 To confirm the AdipoRon-mediated phenotypic shift in AMs, we compared AdipoRon treatment with
188 vehicle in infected and uninfected APN-/- AMs by global RNAseq analysis. In uninfected AMs, more
189 genes were upregulated in response to AdipoRon treatment, while the opposite was observed in AMs
190 after 12 hours post-infection, with AdipoRon treatment associated with gene silencing (**Fig S3A**).
191 Inflammatory/M1-associated gene expression was suppressed by AdipoRon treatment in infected AMs,
192 including *Il1a*, *Il1b*, *Ccl2*, *Cd38*, *Tlr4*, and *Hif1a*, while the anti-inflammatory *Tgfb* was increased, as
193 were autophagy genes, including *Map1lc3a* and *Map1lc3b* genes that are critical for LAP (**Fig. S3B**).
194 In contrast, inflammatory gene expression appeared to be increased by AdipoRon in uninfected AMs.
195 GSEA pathway analysis confirmed inhibition of cytokine signaling by AdipoRon in infected AMs and
196 also identified activation of gene pathways associated with oxidative phosphorylation (**Fig. S3C**), a
197 metabolic pathway favored by M2 macrophages [18]. Our RNAseq results thus confirm an AdipoRon-
198 mediated inhibition of the inflammatory/M1 phenotype of APN-/- AMs in response to fungal infection,
199 and identify a potential role for autophagy induction.

200 Since LAP is an important mechanism of killing of *A. fumigatus* by macrophages [19], we aimed to
201 determine if phagosomal LC3 activation is increased in APN-/- AMs by AdipoRon treatment. Using
202 immunofluorescence microscopy staining of LC3, we observed clear colocalization of LC3 staining
203 and DS-RED+(viable) conidia in AdipoRon-treated APN-/- AMs (**Fig. 7A**), with visibly less
204 colocalization in untreated AMs that was confirmed by image quantification (**Fig. 7B**). The median
205 fluorescence intensity (MFI) of LC3+ macrophage staining was also increased by AdipoRon in both
206 wild-type and APN-/- AMs as measured by flow cytometry (**Fig. 7C**). Collectively, these results
207 demonstrate a role for adiponectin in LAP in AMs in response to *A. fumigatus* conidia.

208 **Discussion**

209 To our knowledge, our study is the first to identify a role for adiponectin in LC3-associated
210 phagocytosis (LAP) in response to infection. Previous studies reported roles for adiponectin in LC3-
211 mediated autophagy in skeletal muscle cells [20,21], cardiomyocytes [22], or macrophages in a mouse
212 model of atherosclerosis [23]. In addition, AM autophagy is critical for prevention of spontaneous lung
213 inflammation driven by airway microflora [24]. Although others have identified a role for the LC3
214 pathway in efferocytosis by macrophages [25], and although adiponectin promotes macrophage
215 efferocytosis [26,27], a direct connection between adiponectin, LC3/autophagy and macrophage
216 efferocytosis is lacking. Since macrophage autophagy and removal of apoptotic cells are important
217 mechanisms to limit lung inflammatory pathology [24,27,28], it will be of interest in future studies to
218 determine their role in adiponectin-mediated dampening of inflammation in IA.

219 A number of studies have defined a critical role for LAP in protection from *A. fumigatus* infection
220 [19,29–31]. LAP dampens inflammation in response to *A. fumigatus* by inhibition of the NLRP3
221 inflammasome and IL-1b via activation of DAPK1 [29]. In our study, we observed that AdipoRon
222 decreased transcription of IL-1α and IL-1β genes in APN-/- AMs. Interestingly, blockade of IL-1
223 receptor signaling (by IL-1ra) restored autophagy/LC3 recruitment in NADPH oxidase-deficient
224 macrophages, a hallmark myeloid cell deficiency of Chronic Granulomatous Disease [32]. Since both
225 AdipoRon and IL-1ra promote LC3 activation, it will be important in future studies to determine if
226 AdipoRon could restore autophagy in NADPH oxidase-deficient macrophages, and to identify shared
227 regulatory pathways.

228 A previous study reported that LAP-associated fungal clearance was inhibited by fungal melanin, a

229 virulence factor of *A. fumigatus* [30]. How APN stimulates LAP in response to *A. fumigatus* and the
230 ability to overcome LAP interference by fungal melanin remain unknown. Furthermore, we observed
231 that chitin inhalation resulted in decreased production of lung adiponectin and AdipoR1 expression in
232 murine airway cells [33]. It will be of interest to determine the effect of AdipoRon on recognition of
233 multiple fungal pathogen-associated molecular patterns by WT and APN pathway-deficient AMs,
234 specifically in the context of LC3 activation.

235 Adiponectin has two canonical signaling receptors with broad, yet different cell/tissue distribution [34].
236 We observed that both AdipoR1 and AdipoR2 contribute to adiponectin-mediated protection from IA
237 and dampening of inflammatory pathology. However, some differences were evident, as AdipoR1-/-
238 mice with IA exhibited the highest levels of lung inflammatory cytokine transcription that was not as
239 clear in AdipoR1-/- AMs, suggesting that immune pathology in AdipoR1-/- mice was not driven solely
240 by the lack of AdipoR1 signaling in AMs, but also by other immune and resident lung cells, with a
241 contribution of potentially enhanced signaling through AdipoR2. AMs express both AdipoRs, and their
242 expression was modulated by *A fumigatus* infection, most significantly for AdipoR1, which was
243 increased in response to infection in WT AMs but decreased in APN-/- AMs. Furthermore, both
244 AdipoR1 and AdipoR2 were required for AdipoRon-mediated improvement in *A. fumigatus* killing, as
245 AdipoRon was not effective in AdipoR1/R2-/- AMs, confirming a role for both receptors in APN-
246 mediated enhancement of AM function. However, the relative contribution of AdipoR-expressing
247 AMs in adiponectin-mediated protection from infection remains unclear, and thus remains a subject of
248 future investigation.

249 AMs are dynamic cells, and their activation and polarization falls on a spectrum from M1 to M2, as
250 these are designations and not indicative of a static phenotype [35,36]. In our study, AM treatment with
251 AdipoRon decreased expression of M1 genes and activated M2 genes in *A. fumigatus*-infected APN-/-
252 AMs, although these phenotypes are not identical to previously published studies using classical
253 activation stimuli, such as LPS/IFNg for M1 and IL-4 for M2 [37,38]. It is thus more appropriate to
254 refer to APN-/- AMs as 'M1-like' and AdipoRon-treated AMs as 'M2-like' cells [39,40]. Perhaps more
255 importantly, AdipoRon treatment of APN-/- AMs resulted in activation of genes associated with
256 oxidative phosphorylation that is associated with M2-like macrophages, in contrast to glycolysis-
257 favoring M1 macrophages [18]. In support of increased oxidative metabolism for AdipoRon-treated
258 APN-/- AMs, arginase-2 (*Arg2*) expression was also increased, and mitochondrial *Arg2* was recently

259 identified as critical for induction of oxidative phosphorylation in inflammatory macrophages [41].
260 Collectively, the results of our study confirm a role for APN in skewing AMs toward an M2-like
261 phenotype.

262 Obesity is widely accepted as an inflammatory disease characterized by adipose tissue inflammation
263 and decreased APN and APN receptor expression [6,42–45], yet the effect of obesity-related APN
264 pathway-inhibition in response to *A. fumigatus* infection is not known. In response to infection with
265 *Listeria monocytogenes*, both obese and APN-/- mice exhibited attenuated clearance that was
266 characterized by an inflammatory phenotype in bone marrow macrophages that was partially restored
267 by AdipoRon [7]. Furthermore, obesity is associated with an increased inflammatory phenotype in
268 alveolar macrophages [46]. It is therefore possible that stimulation of the APN pathway with AdipoRon
269 will improve AM killing of *A. fumigatus* in obese mice, an outcome that would support the APN
270 pathway as a potential therapeutic route in IA patients with low APN levels.

Acknowledgements

We would like to thank Azriel Manalaysay, Alsace Key, and Gwen Schmiedel for assistance with animal care and genetic screening, Brielle Batch for technical assistance, Takuya Akiyama for assistance with confocal microscopy, Americo Lopez-Yglesias for assistance with flow cytometry, and Tobias Hohl for review of this manuscript. The study was supported by National Institutes of Health NIH R21AI163574 (ST) and T32 AI060519 (NBA; IUSM Department of Microbiology and Immunology, American Lung Association Innovation Award #IA-690880 (ST), and the Indiana Clinical and Translational Sciences Institute, funded in part by grant # UM1TR004402 from the National Institutes of Health, National Center for Advancing Translational Sciences, Clinical and Translational Science Award (ST).

Author contributions

Conceptualization, S.P.T., H.G., J.L.; Methodology, J.L. and H.G.; Investigation. H.G., J.L., and N.B.A.; Resource; J.L., N.B.A., and H.G.; Writing - S.PT, J.L and H.G.; Visualization, H.G, J.L.; Funding Acquisition. S.P.T.

Declaration of Interests

The authors declare no competing interests.

KEY RESOURCES TABLE

REAGENT or RESOURCE	SOURCE	IDENTIFIER
Antibodies		
CD45-PerCP	BD Biosciences	557235
SiglecF-Superbright600	Thermo Fisher Scientific	63-1702-82
SiglecF-PE	BD Biosciences	552126
Cd11c-SparekBlue550	BioLegend	117366
Cd11c-PECy7	Thermo Fisher Scientific	25-0114-81
Ly6G-BV785	BioLegend	127645
Ly6G-FITC	BD Biosciences	551460
Fc Block	BD Biosciences	553142

Rabbit IgG - Isotype control	Abcam	ab171870
Anti-AdipoR1 antibody	Abcam	ab70362
Goat anti-Rabbit IgG H&L (Alexa Fluor 405)	Abcam	ab175652
Anti-mouse EGR2	Invitrogen	247632
Anti-mouse CD38	Invitrogen	2504972
Goat anti-Rabbit IgG (H+L) Cross-Adsorbed Secondary Antibody, Alexa Fluor 488	Thermo Fisher Scientific	A-11008
Adiponectin receptor 1 Recombinant Rabbit Monoclonal Antibody	Invitrogen	MA5-32249
Chemicals		
Streptavidin, Alexa Fluor 633 conjugate	Invitrogen	S21375
Biotin-XX, SSE	Invitrogen	B6352, B1606
ACK lysing buffer	Thermo Fisher Scientific	A1049201
Hygromycin B, *Streptomyces* sp.	Calbiochem	31282-04-9
Xylene	Millipore Sigma	XX0060
TRIzol reagent	Thermo Fisher Scientific	15596026
AdipoRon	Cayman chemical	924416-43-3
Albumin, Bovine Serum	Millipore Sigma	126579
Normal Donkey Serum	abcam	ab7475
Sodium Bicarbonate 7.5% solution	Thermo Fisher Scientific	25080094
Carboxymethylcellulose sodium salt	Thermo Fisher Scientific	A18105.36
0.5 M EDTA	Thermo Fisher Scientific	15575020
Dimethyl Sulfoxide	Millipore Sigma	D4540
10% Neutral Buffered Formalin	Thermo Fisher Scientific	5701
RPMI 1640, 1X with L-glutamine	CORNING	28121001
2-Mercaptoehanol	A ALDRICH	SHBF0971V
50ug Murine GM-CSF	PeproTech	032255 K1622
Lipofectamine 2000 Transfection Reagent	Thermo Fisher Scientific	11668019
Vectashield mounting medium for fluorescence with DAPI	VECTOR laboratories	H-1200-10

FluoSpheres Polystyrene Microspheres, 1.0 µm, red fluorescent (580/605), for tracer studies	Thermo Fisher Scientific	F13083
Critical commercial assays		
Silver stain (Modified GMS)	Millipore Sigma	HT100A
RNeasy Mini kit	Qiagen	74106
RNase-Free DNase set	Qiagen	79256
PowerUp SYBR Green Master Mix	Thermo Fisher Scientific	A25742
ABsolute Blue qPCR low ROX mix	Thermo Fisher Scientific	AB-4318
High Capacity cDNA Reverse Transcription Kit	Thermo Fisher Scientific	4368814
Mouse Adiponectin/Acrp30 ELISA kit	R&D Systems	DY1119
Murine TNF-α Standard TMB ELISA kit	Peprotech	900-T54
LC3B Antibody Kit for Autophagy	Invitrogen	L10382
TriFECTa RNAi Kit	Integrated DNA Technologies	N/A
Experimental models: Organism/strains		
A. fumigatus strain AF293	Fungal Genetic Stock Center	Cat#A1100
A. fumigatus strain AF293 ds-Red (FLARE strain)	Jhingran et al. [24w]	N/A
Oligonucleotides		
18S rRNA-encoding DNA primers and probe	50-/56-FAM/AGC CAG CGG/ZEN/CCC GCAAAT G/3IABkFQ/-30	
Software and algorithms		
FlowJo	FlowJo 10	N/A
Prism 9	Prism 9	N/A
Gen5	BioTek	N/A
Image J	Image J	N/A

288 **RESOURCE AVAILABILITY**

289 **Lead contact**

290 Further information and requests for resources and reagents should be directed to and will be fulfilled
291 by the lead contact, Steven P. Templeton. (sptemple@iu.edu)

292 **Material Availability**

293 All materials within the paper are available from the corresponding author upon reasonable request.

294 This study did not generate new reagents.

295 **Data and Code Availity**

296 The RNAseq data are available at Gene Expression Omnibus (Accession #GSE268782).

297 **Materials and Methods**

298 **Mice**

299 C57BL/6 and adiponectin-deficient (*Adipoq*−/−) and *AdipoR2*+/− mice were obtained from The
300 Jackson Laboratory, while AdipoR1+/- mice were obtained from the Mutant Mouse Resource and
301 Research Center (MMRRC). To obtain homozygous deletion mice for *AdipoR1*−/−, and *AdipoR2*−/−
302 mice, heterozygous mice were breed with F1 animals heterozygous and offspring were screened by
303 PCR, with loss of protein confirmed in a subset of animals by flow cytometry. All animal handling and
304 experimental procedures were performed in accordance with the recommendations found in the Guide
305 for the Care and Use of Laboratory Animals of the National Institutes of Health. The work in this study
306 was approved by the Institutional Animal Care and Use Committee of the host campus of Indiana
307 University School of Medicine-Terre Haute, Indiana State University.

308 **Fungal strains and cultivation**

309 The clinical isolates AF293 was previously obtained from the Fungal Genetics Stock Center and grown
310 on Malt Extract Agar plates at 22˚C. To generate FLARE conidia, AF293-dsRed conidia (provided by
311 Dr. Tobias Hohl, Memorial Sloan-Kettering) were rotated in 0.5 mg/ml Biotin XX, SSE in 1 ml of 50
312 mM $NaHCO_3$ for 2 h at 4˚C, washed with 0.1 M Tris-HCl (pH 8.0), incubated with 0.02 mg/ml Af633-
313 streptavidin for 30 min at RT, and resuspended in PBS for use [47].

314 **Fungal aspiration and infection**

315 Neutrophils were depleted by i.p. injection of 0.5 mg of α-Ly6G (1A8 clone) 24 h pre- and post-
316 infection for invasive pulmonary aspergillosis mice model, as described [8]. Isoflurane-anesthetized
317 mice involuntarily aspirated 50 µl of suspension including $1 – 2 \times 10^7$ of conidia. For survival test,
318 infected mice were monitored for 8 days post infection. For further analyses, a subset of infected mice
319 were euthanized with sodium pentobarbital and mouse BAL cells and lungs were harvested 24 h or 72
320 h later for further analyses.

321 **Histology**

322 At 3 days post infection, lungs were harvested after perfusion with 5 ml of PBS followed with 5 ml of
323 10 % phosphate buffered formalin and inflated with formalin. Lung tissue was embedded in parafilm
324 after dehydration and sectioned in 4 µm slices using xylene and ethanol and stained with modified
325 Gomori modified methanamine silver (GMS) and hematoxylin and eosin (H&E) staining [8].
326 Quantification of GMS staining to determine fungal burden was performed as previously described
327 [48].

328 **Quantitative PCR fungal burden assay**

329 At 72 h post infection, lungs were harvested, frozen in liquid nitrogen and lyophilized. Genomic DNA
330 was extracted from homogenized lung tissue with DNA extraction buffer for *Aspergillus* nucleic acids
331 and subsequent phenol/chloroform extraction. Quantitative PCR (qPCR) fungal burden assay was
332 performed using 0.2 µg of genomic DNA with 18S rRNA-encoding DNA primers and probe sets with a
333 modified probe quencher (50-/56-FAM/AGC CAG CGG/ZEN/CCC GCAAAT G/3IABkFQ/-30) [49].
334 qPCR was performed using the CFX Connect Real-Time System. Threshold values were used to
335 calculate the corresponding fungal DNA content in the lung tissues.

336 **Tissue RNA extraction and gene expression analysis**

337 Total RNA was extracted from homogenized lungs in TRIzol reagent. Following the upper phase,
338 further RNA purification was performed using a Qiagen RNeasy column and DNase treatment per the
339 manufacturer's recommendations [50]. Mouse β-actin was used as the housekeeping gene for cytokine
340 analysis in the murine model. Most primers were designed using the Primer3 software (version 0.4.0)
341 from the whole sequence available in GenBank.

342 **BALF Flow cytometric analysis**

343 BALF cell composition was determined by flow cytometric analysis with staining of surface markers.
344 In brief, BALF was centrifuged and the cell pellet was washed with 1 ml of FACS buffer (PBS, 5%
345 FBS, 50 mM EDTA). The washed pellet was lysed of red blood cells with ACK lysis buffer and stained
346 with 10% rat serum, Fc receptor blocking Ab, and antibodies: rat anti-mouse Ly6G-FITC or -BV785,
347 rat anti-mouse SiglecF-PE or -Superbright600, rat anti-mouse CD45-PerCP, and rate anti-mouse
348 CD11c-PE-Cy7 or -SparkBlue550 [50,51]. For staining of AdipoR1, the washed pellet was
349 resuspended in blocking solution containing 10% donkey serum, Fc receptor blocking Ab, and 1%
350 Bovine serum albumin in PBS for 30 min, incubated with the primary AdipoR1 antibody for 1 h and
351 incubated with the IgG secondary antibodies [33]. Analyses were performed by flow cytometric
352 analysis on a Guava EasyCyte HT system and Cytek. Flow cytometric data were analyzed using
353 FlowJo software.

354 **BALF ELISA analysis**

355 Serum and BALF supernatants were collected after centrifugation. ELISA analyses were performed for
356 TNF-α cytokine (PeproTech) and Adiponectin (R&D Systems) as described by the manufacturer's
357 protocol.

358 **Alveolar macrophage extraction and culture**

359 Seven to 8 weeks old mice were euthanized, and an 18-gauge catheter was inserted into the trachea and
360 alveolar macrophages were harvested from mouse lungs with sterile filtered PBS containing 2 mM
361 EDTA (diluted 1:250 from 0.5 M EDTA stock solution) and 0.5% Fetal bovine serum (FBS) in 5ml
362 BAL fluid. Cells were separated from the BALF by centrifugation at 400 × *g* for 6 min at 4°C and the
363 cells were suspended in RPMI 1640 supplemented with penicillin (100 U/ml), streptomycin (100
364 U/ml), 5% heat-inactivated FBS, 20ng/ml GM-CSF and 143mM beta-mercaptoethanol. BALF cells
365 were plated in Corning Costar Flat Bottom 12 well Cell Culture Plates at a concentration of 5 ×
366 10^5 cells per well. The cells were allowed to adhere for 24 hours at 37°C under a humidified
367 atmosphere with 5% CO2 and were washed with PBS thrice and cell culture media was added,
368 allowing only the adherent AMs to culture in the wells. The cell culture media was changed on day 3,
369 day 6 and day 9 of the cultures. AMs were fully confluent and ready for treatment and infection on day
370 10. The wells for divided into DMSO control, AdipoRon treatment with AF293/FLARE infection and

371 AF293/FLARE infection groups.

372 **Quantitative RT-PCR for ex-vivo gene expression analysis**

373 AMs were treated with 20 uM AdipoRon or vehicle-treated for 24 hours, followed by infection with
374 AF293 fixed and swollen conidia using RPMI 1640 medium at a concentration of 9 conidia per cell for
375 RT-PCR. After 10 hours of infection, cells were ready for RNA extraction and cDNA synthesis. RNA
376 extraction from AMs was done using Qiagen RNeasy Mini kit, following the manufacturer's protocol.

377 **AM supernatant ELISA**

378 After culturing for 10 days, AMs were grouped into uninfected, vehicle (DMSO), infected and
379 AdipoRon + infected groups. After the infection at a concentration of 9 conidia per cell with fixed and
380 swollen AF293 conidia for 10 hours, the supernatants were collected and analyzed for TNF-alpha
381 expression.

382 **AM flow cytometric analysis**

383 **FLARE uptake and killing**

384 Conidia was harvested from 7-10 days old Minimal Media (GMM) plates. AF293-dsRed conidia were
385 rotated in 0.5 mg/ml Biotin XX, SSE in 1 ml of 50 mM NaHCO3 for 2 h at 4˚C, washed with 0.1 M
386 Tris-HCl (pH 8.0), incubated with 0.02 mg/ml Af633-streptavidin for 30 min at RT, and resuspended in
387 PBS for use. For in-vitro conidial uptake and killing assays, $5x10^5$ FLARE conidia were added to $5x10^5$
388 alveolar macrophages (1:1). After 10 hours alveolar macrophages were harvested using cell scraper
389 with slight force from the wells in 500 ul ice cold FACS buffer per well and centrifuged at 400 × *g* for
390 6 min at 4°C. The cell pellet was washed with 1 ml of FACS buffer (PBS, 5% FBS, 50 mM EDTA)
391 and the samples were passed through 70µm filter to clear hyphae and have clear sample. The cells were
392 analyzed by the flow cytometry for dsRed (Ex/Em: 558nm/583nm) and AF633 (Ex/Em:
393 631nm/650nm) fluorescence followed by gating using FlowJo.

394 **M1/M2 phenotype study**

395 For M1/M2 phenotype analysis cells were stained with 10% rat serum, Fc receptor blocking Ab and
396 antibody: *CD38 Monoclonal Antibody (90), APC-eFluor™ 780, eBioscience™* for 15 min at room
397 temperature. For staining with the antibody: *EGR2 Monoclonal Antibody (erongr2), PE-Cyanine7,*

398 *eBioscience*™ cells were permeabilized using Cytoperm and processed for staining.

399 **AM Microscopy**

400 **FLARE uptake and killing**

401 Alveolar macrophages were plated in Cellvis 35 mm Glass bottom dish with 14 mm micro-well and
402 were infected with FLARE/DsRed at a 1:1 ratio. Cells were live imaged after 6 hours on a ZEISS
403 LSM780 confocal microscopy.

404 **LC3 phagocytosis assay**

405 On day 10, cells were treated with 20 uM AdipoRon for 24 hours followed by treatment with 90µm
406 chloroquine for 13 hours. Cells were then infected with DsRed+ conidia for 120 min and then fixed
407 with 3.7% formaldehyde in PBS for 15 min at room temperature. LC3B antibody kit for autophagy was
408 used and the manufacturer's protocol is followed for LC3 staining. Invitrogen™ Goat anti-Rabbit IgG
409 (H+L) Cross-Adsorbed Secondary, Antibody, Alexa Fluor™ 488 has been used for secondary staining.
410 Cells were washed and counter stained with DAPI using VECTASHIELD® Antifade Mounting
411 Medium has been done. Microscopy was performed on OLYMPUS IX83 and analyzed as follows:
412 nucleus: DAPI, LC3b: FITC, conidia: Cy5 channel at 20X.

413 **siRNA knockdown of *Adipor1***

414 TriFECTa RNAi Kit was used with Lipofectamine 2000 reagent for transfection. Adherent 10 days old
415 alveolar macrophages were treated with diluted AdipoR1 SiRNA in Lipofectamine (1:1 ratio) at 1nM
416 per 5 x 10^5 cells concentration for 72 hours. The cells were then quantified for AdipoR1 receptor
417 expression using AdipoR1 RT-PCR and compared with provided positive and negative controls.

418 **STATISTICAL ANALYSIS**

419 Prism software was used for generation of figures and for statistical analyses (GraphPad). Unpaired *t*
420 tests or ANOVA tests were used to measure statistical significance. Differences between experimental
421 groups that resulted in a p value < 0.05 were considered significant.

422

423

424 **References**

425 1. Veerdonk FL Van De, Gresnigt MS, Romani L, Netea MG, Latgé JP. Aspergillus fumigatus morphology
426 and dynamic host interactions. Nature Reviews Microbiology 2017 15:11. 2017;15: 661–674.
427 doi:10.1038/nrmicro.2017.90

428 2. Carvalho A, Cunha C, Iannitti RG, Luca A De, Giovannini G, Bistoni F, et al. Inflammation in aspergillosis:
429 the good, the bad, and the therapeutic. Ann N Y Acad Sci. 2012;1273: 52–59. doi:10.1111/J.1749-
430 6632.2012.06754.X

431 3. Sprenkeler EGG, Gresnigt MS, van de Veerdonk FL. LC3-associated phagocytosis: a crucial mechanism
432 for antifungal host defence against Aspergillus fumigatus. Cell Microbiol. 2016;18: 1208–1216.
433 doi:10.1111/CMI.12616

434 4. Hoffstedt J, Arvidsson E, Sjölin E, Wåhlén K, Arner P. Adipose tissue adiponectin production and
435 adiponectin serum concentration in human obesity and insulin resistance. J Clin Endocrinol Metab.
436 2004;89: 1391–1396. doi:10.1210/JC.2003-031458

437 5. Ren Y, Zhao H, Yin C, Lan X, Wu L, Du X, et al. Adipokines, Hepatokines and Myokines: Focus on Their
438 Role and Molecular Mechanisms in Adipose Tissue Inflammation. Front Endocrinol (Lausanne). 2022;13.
439 doi:10.3389/FENDO.2022.873699

440 6. Arita Y, Kihara S, Ouchi N, Takahashi M, Maeda K, Miyagawa JI, et al. Paradoxical decrease of an
441 adipose-specific protein, adiponectin, in obesity. Biochem Biophys Res Commun. 1999;257: 79–83.
442 doi:10.1006/BBRC.1999.0255

443 7. Masamoto Y, Arai S, Sato T, Yoshimi A, Kubota N, Takamoto I, et al. Adiponectin enhances antibacterial
444 activity of hematopoietic cells by suppressing bone marrow inflammation. Immunity. 2016;44: 1422–
445 1433. doi:10.1016/j.immuni.2016.05.010

446 8. Amarsaikhan N, Tsoggerel A, Hug C, Templeton SP. The metabolic cytokine adiponectin inhibits
447 inflammatory lung pathology in invasive aspergillosis. J Immunol. 2019;203: 956–963.
448 doi:10.4049/JIMMUNOL.1900174

449 9. Bhatia S, Fei M, Yarlagadda M, Qi Z, Akira S, Saijo S, et al. Rapid host defense against Aspergillus
450 fumigatus involves alveolar macrophages with a predominance of alternatively activated phenotype.
451 PLoS One. 2011;6. doi:10.1371/journal.pone.0015943

452 10. Chignard M, Balloy V, Sallenave JM, Si-Tahar M. Role of Toll-like receptors in lung innate defense

453 against invasive aspergillosis. Distinct impact in immunocompetent and immunocompromized hosts.
454 Clin Immunol. 2007;124: 238–243. doi:10.1016/J.CLIM.2007.05.004

455 11. Kubota N, Terauchi Y, Yamauchi T, Kubota T, Moroi M, Matsui J, et al. Disruption of adiponectin causes
456 insulin resistance and neointimal formation. J Biol Chem. 2002;277: 25863–25866.
457 doi:10.1074/JBC.C200251200

458 12. Ke M, Cabrero A, Saha PK, Kojima H, Li L, Chang BHJ, et al. Increased beta -oxidation but no insulin
459 resistance or glucose intolerance in mice lacking adiponectin. J Biol Chem. 2002;277: 34658–34661.
460 doi:10.1074/JBC.C200362200

461 13. Maeda N, Shimomura I, Kishida K, Nishizawa H, Matsuda M, Nagaretani H, et al. Diet-induced insulin
462 resistance in mice lacking adiponectin/ACRP30. Nat Med. 2002;8: 731–737. doi:10.1038/NM724

463 14. Jablonski KA, Amici SA, Webb LM, Ruiz-Rosado JDD, Popovich PG, Partida-Sanchez S, et al. Novel
464 Markers to Delineate Murine M1 and M2 Macrophages. PLoS One. 2015;10.
465 doi:10.1371/JOURNAL.PONE.0145342

466 15. Jhingran A, Mar KB, Kumasaka DK, Knoblaugh SE, Ngo LY, Segal BH, et al. Tracing conidial fate and
467 measuring host cell antifungal activity using a reporter of microbial viability in the lung. Cell Rep.
468 2012;2: 1762. doi:10.1016/J.CELREP.2012.10.026

469 16. Okada-Iwabu M, Yamauchi T, Iwabu M, Honma T, Hamagami K-I, Matsuda K, et al. A small-molecule
470 AdipoR agonist for type 2 diabetes and short life in obesity. Nature. 2013;503. doi:10.1038/nature12656

471 17. Salvator H, Grassin-Delyle S, Brollo M, Couderc LJ, Abrial C, Victoni T, et al. Adiponectin inhibits the
472 production of TNF-α, IL-6 and chemokines by human lung macrophages. Front Pharmacol. 2021;12:
473 718929. doi:10.3389/FPHAR.2021.718929

474 18. Viola A, Munari F, Sánchez-Rodríguez R, Scolaro T, Castegna A. The Metabolic Signature of Macrophage
475 Responses. Front Immunol. 2019;10. doi:10.3389/FIMMU.2019.01462

476 19. Sprenkeler EGG, Gresnigt MS, van de Veerdonk FL. LC3-associated phagocytosis: a crucial mechanism
477 for antifungal host defence against Aspergillus fumigatus. Cell Microbiol. 2016;18: 1208–1216.
478 doi:10.1111/CMI.12616

479 20. Gamberi T, Modesti A, Magherini F, D'Souza DM, Hawke T, Fiaschi T. Activation of autophagy by
480 globular adiponectin is required for muscle differentiation. Biochim Biophys Acta. 2016;1863: 694–702.
481 doi:10.1016/J.BBAMCR.2016.01.016

482 21. Liu Y, Palanivel R, Rai E, Park M, Gabor T V., Scheid MP, et al. Adiponectin stimulates autophagy and
483 reduces oxidative stress to enhance insulin sensitivity during high-fat diet feeding in mice. Diabetes.
484 2015;64: 36–48. doi:10.2337/DB14-0267

485 22. Essick EE, Wilson RM, Pimentel DR, Shimano M, Baid S, Ouchi N, et al. Adiponectin modulates oxidative
486 stress-induced autophagy in cardiomyocytes. PLoS One. 2013;8. doi:10.1371/JOURNAL.PONE.0068697

487 23. Li C, Wang Z, Wang C, Ma Q, Zhao Y. Perivascular adipose tissue-derived adiponectin inhibits collar-
488 induced carotid atherosclerosis by promoting macrophage autophagy. PLoS One. 2015;10.
489 doi:10.1371/JOURNAL.PONE.0124031

490 24. Kanayama M, He Y-W, Shinohara ML. The lung is protected from spontaneous inflammation by
491 autophagy in myeloid cells. J Immunol. 2015;194: 5465–5471. doi:10.4049/JIMMUNOL.1403249

492 25. Asare PF, Roscioli E, Hurtado PR, Tran HB, Mah CY, Hodge S. LC3-Associated Phagocytosis (LAP): A
493 Potentially Influential Mediator of Efferocytosis-Related Tumor Progression and Aggressiveness. Front
494 Oncol. 2020;10. doi:10.3389/FONC.2020.01298

495 26. Galvan MD, Hulsebus H, Heitker T, Zeng E, Bohlson SS. Complement protein C1q and adiponectin
496 stimulate Mer tyrosine kinase-dependent engulfment of apoptotic cells through a shared pathway. J
497 Innate Immun. 2014;6: 780–792. doi:10.1159/000363295

498 27. Tee JH, Vijayakumar U, Shanmugasundaram M, Lam TYW, Liao W, Yang Y, et al. Isthmin-1 attenuates
499 allergic Asthma by stimulating adiponectin expression and alveolar macrophage efferocytosis in mice.
500 Respir Res. 2023;24. doi:10.1186/S12931-023-02569-1

501 28. Madenspacher JH, Morrell ED, Gowdy KM, McDonald JG, Thompson BM, Muse G, et al. Cholesterol 25-
502 hydroxylase promotes efferocytosis and resolution of lung inflammation. JCI Insight. 2020;5.
503 doi:10.1172/JCI.INSIGHT.137189

504 29. Oikonomou V, Moretti S, Renga G, Galosi C, Borghi M, Pariano M, et al. Noncanonical Fungal Autophagy
505 Inhibits Inflammation in Response to IFN-γ via DAPK1. Cell Host Microbe. 2016;20: 744–757.
506 doi:10.1016/J.CHOM.2016.10.012

507 30. Akoumianaki T, Kyrmizi I, Valsecchi I, Beauvais A, Latge J-P, Chamilos G. Aspergillus cell wall melanin
508 blocks LC3-associated phagocytosis to promote pathogenicity. Cell Host Microbe. 2016;19: 79–90.
509 doi:10.1016/j.chom.2015.12.002

510 31. Kyrmizi I, Ferreira H, Carvalho A, Figueroa JAL, Zarmpas P, Cunha C, et al. Calcium sequestration by

511 fungal melanin inhibits calcium-calmodulin signalling to prevent LC3-associated phagocytosis. Nat
512 Microbiol. 2018;3: 791–803. doi:10.1038/S41564-018-0167-X

513 32. De Luca A, Smeekens SP, Casagrande A, Iannitti R, Conway KL, Gresnigt MS, et al. IL-1 receptor blockade
514 restores autophagy and reduces inflammation in chronic granulomatous disease in mice and in humans.
515 Proc Natl Acad Sci U S A. 2014;111: 3526–3531. doi:10.1073/PNAS.1322831111

516 33. Amarsaikhan N, Stolz DJ, Wilcox A, Sands EM, Tsoggerel A, Gravely H, et al. Reciprocal inhibition of
517 adiponectin and innate lung immune responses to chitin and *Aspergillus fumigatus*. Front Immunol.
518 2019;10: 1057. doi:10.3389/FIMMU.2019.01057

519 34. Yamauchi T, Kadowaki T. Adiponectin receptor as a key player in healthy longevity and obesity-related
520 diseases. Cell Metab. 2013;17: 185–196. doi:10.1016/J.CMET.2013.01.001

521 35. Hu G, Christman JW. Editorial: Alveolar Macrophages in Lung Inflammation and Resolution. Front
522 Immunol. 2019;10. doi:10.3389/FIMMU.2019.02275

523 36. Byrne AJ, Mathie SA, Gregory LG, Lloyd CM. Pulmonary macrophages: key players in the innate defence
524 of the airways. Thorax. 2015;70: 1189–1196. doi:10.1136/THORAXJNL-2015-207020

525 37. Orecchioni M, Ghosheh Y, Pramod AB, Ley K. Macrophage Polarization: Different Gene Signatures in
526 M1(LPS+) vs. Classically and M2(LPS-) vs. Alternatively Activated Macrophages. Front Immunol. 2019;10.
527 doi:10.3389/FIMMU.2019.01084

528 38. Colombo G, Pessolano E, Talmon M, Genazzani AA, Kunderfranco P. Getting everyone to agree on gene
529 signatures for murine macrophage polarization in vitro. PLoS One. 2024;19.
530 doi:10.1371/JOURNAL.PONE.0297872

531 39. Yunna C, Mengru H, Lei W, Weidong C. Macrophage M1/M2 polarization. Eur J Pharmacol. 2020;877.
532 doi:10.1016/J.EJPHAR.2020.173090

533 40. Parisi L, Gini E, Baci D, Tremolati M, Fanuli M, Bassani B, et al. Macrophage Polarization in Chronic
534 Inflammatory Diseases: Killers or Builders? J Immunol Res. 2018;2018. doi:10.1155/2018/8917804

535 41. Dowling JK, Afzal R, Gearing LJ, Cervantes-Silva MP, Annett S, Davis GM, et al. Mitochondrial arginase-2
536 is essential for IL-10 metabolic reprogramming of inflammatory macrophages. Nat Commun. 2021;12.
537 doi:10.1038/S41467-021-21617-2

538 42. Steffes MW, Gross MD, Schreiner PJ, Yu X, Hilner JE, Gingerich R, et al. Serum adiponectin in young
539 adults - Interactions with central adiposity, circulating levels of glucose, and insulin resistance: The

540 CARDIA study. Ann Epidemiol. 2004;14: 492–498. doi:10.1016/j.annepidem.2003.10.006

541 43. Sood A, Shore SA. Adiponectin, Leptin, and Resistin in Asthma: Basic Mechanisms through Population
542 Studies. J Allergy (Cairo). 2013;2013: 1–15. doi:10.1155/2013/785835

543 44. Ghigliotti G, Barisione C, Garibaldi S, Fabbi P, Brunelli C, Spallarossa P, et al. Adipose tissue immune
544 response: Novel triggers and consequences for chronic inflammatory conditions. Inflammation. Springer
545 New York LLC; 2014. pp. 1337–1353. doi:10.1007/s10753-014-9914-1

546 45. Kadowaki T, Yamauchi T. Adiponectin and adiponectin receptors. Endocr Rev. 2005;26: 439–451.
547 doi:10.1210/ER.2005-0005

548 46. Sharma S, Malur A, Marshall I, Huizar I, Barna BP, Pories W, et al. Alveolar macrophage activation in
549 obese patients with obstructive sleep apnea. Surgery. 2012;151: 107–112.
550 doi:10.1016/J.SURG.2011.06.035

551 47. Jhingran A, Kasahara S, Hohl T. Flow Cytometry of Lung and Bronchoalveolar Lavage Fluid Cells from
552 Mice Challenged with Fluorescent Aspergillus Reporter (FLARE) Conidia. Bio Protoc. 2016;6.
553 doi:10.21769/bioprotoc.1927

554 48. Stolz DJ, Sands EM, Amarsaikhan N, Tsoggerel A, Templeton SP. Histological quantification to determine
555 lung fungal burden in experimental aspergillosis. JoVE (Journal of Visualized Experiments). 2018;2018:
556 e57155–e57155. doi:10.3791/57155

557 49. Bhattacharya S, Amarsaikhan N, Maupin AJ, Schlosser A, Füchtbauer E-M, Holmskov U, et al. FIBCD1
558 deficiency decreases disease severity in a murine model of invasive pulmonary aspergillosis.
559 Immunohorizons. 2021;5: 983–993. doi:10.4049/IMMUNOHORIZONS.2100092

560 50. Amarsaikhan N, Sands EM, Shah A, Abdolrasouli A, Reed A, Slaven JE, et al. Caspofungin increases
561 fungal chitin and eosinophil and γδ T Cell-dependent pathology in invasive aspergillosis. J Immunol.
562 2017;199: 624–632. doi:10.4049/JIMMUNOL.1700078

563 51. Lim JY, Jung YE, Hwang HE, Kim CH, Basaran-Akgul N, Goli SH, et al. Survival Factor A (SvfA) Contributes
564 to Aspergillus nidulans Pathogenicity. J Fungi (Basel). 2023;9. doi:10.3390/JOF9020143

565 52. Dobin A, Davis CA, Schlesinger F, Drenkow J, Zaleski C, Jha S, et al. STAR: ultrafast universal RNA-seq
566 aligner. Bioinformatics. 2013;29: 15–21. doi:10.1093/BIOINFORMATICS/BTS635

567 53. Liao Y, Smyth GK, Shi W. featureCounts: an efficient general purpose program for assigning sequence
568 reads to genomic features. Bioinformatics. 2014;30: 923–930. doi:10.1093/BIOINFORMATICS/BTT656

569 54. Robinson MD, McCarthy DJ, Smyth GK. edgeR: a Bioconductor package for differential expression
570 analysis of digital gene expression data. Bioinformatics. 2010;26: 139–140.
571 doi:10.1093/BIOINFORMATICS/BTP616

572 55. McCarthy DJ, Chen Y, Smyth GK. Differential expression analysis of multifactor RNA-Seq experiments
573 with respect to biological variation. Nucleic Acids Res. 2012;40: 4288–4297. doi:10.1093/NAR/GKS042

574 56. Yu G, Wang LG, Han Y, He QY. clusterProfiler: an R package for comparing biological themes among
575 gene clusters. OMICS. 2012;16: 284–287. doi:10.1089/OMI.2011.0118

576 57. Wu T, Hu E, Xu S, Chen M, Guo P, Dai Z, et al. clusterProfiler 4.0: A universal enrichment tool for
577 interpreting omics data. Innovation (Cambridge (Mass)). 2021;2. doi:10.1016/J.XINN.2021.100141

578

579

580

Figure 1.

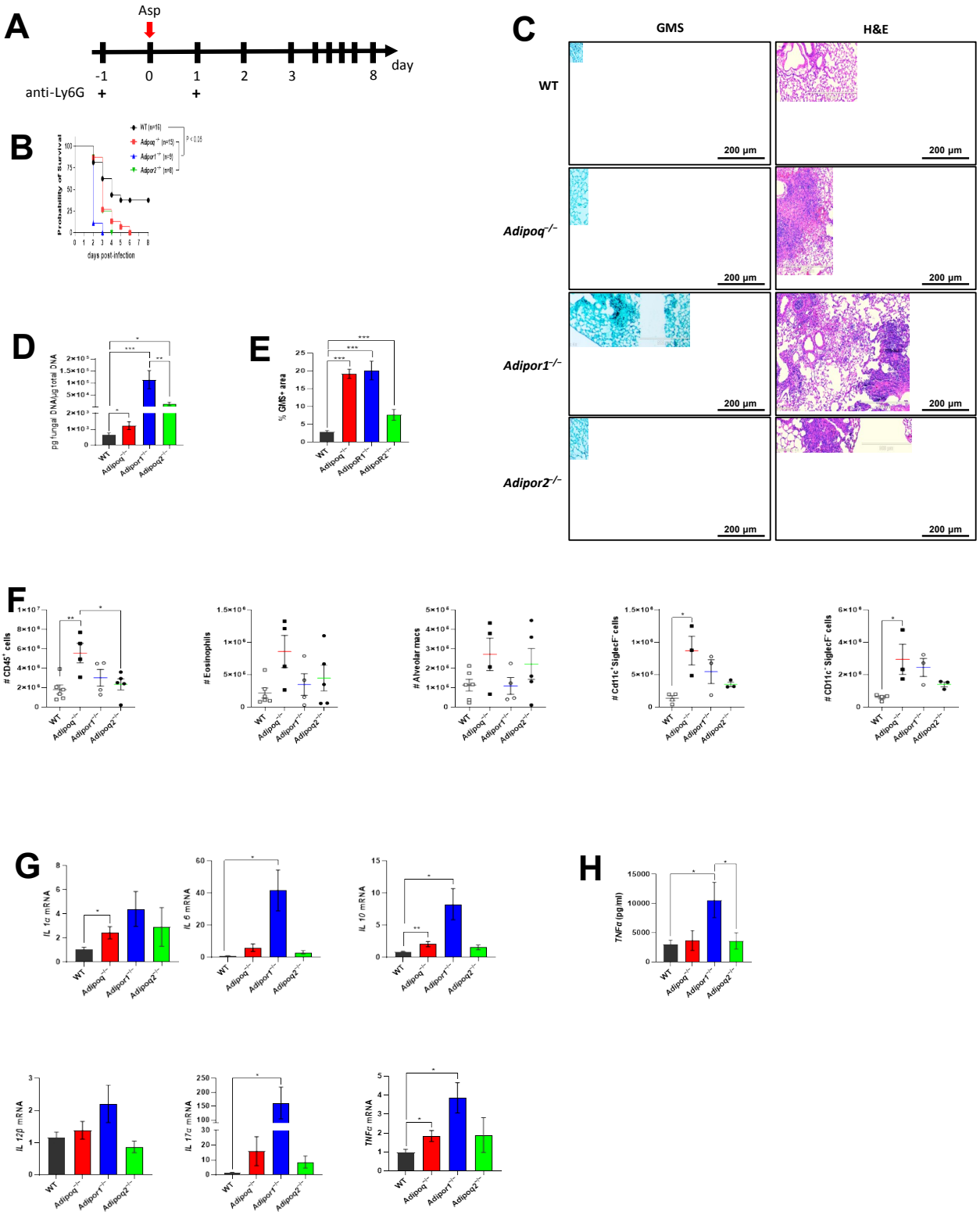
A
Asp
-1
0
1
2
3
8
day
anti-Ly6G
+
+
B
Probability of Survival
days post-infection
C
GMS
H&E
WT
Adipoq-/-
Adipor1-/-
Adipor2-/-
200 µm
D
pg fungal DNA/µg total DNA
E
% GMS+ area
F
CD45+ cells
Eosinophils
Alveolar macs
Cd11c+ SiglecF- cells
CD11c+ SiglecF- cells
G
IL 1α mRNA
IL 6 mRNA
IL 10 mRNA
IL 12β mRNA
IL 17α mRNA
TNFα mRNA
H
TNFα (pg/ml)

582 **Figure 1. Increased mortality, fungal burden, and inflammation in APN pathway-deficient mice**
583 **with invasive aspergillosis.**

584 Wild-type (C57BL/6), APN-/- (*Adipoq*$^{-/-}$), *AdipoR1*$^{-/-}$, and *AdipoR2*$^{-/-}$ mice were neutrophil-depleted
585 and involuntarily aspirated a suspension of *A. fumigatus* conidia and followed for survival or sacrificed
586 on day 3 post-infection as described in Materials and Methods.

587 A. Experimental time course for neutropenic mouse model of infection.
588 B. Survival. *N* = 8-16 mice per group.
589 C. Representative GMS and H&E lung sections.
590 D. Fungal burden determined by quantitative PCR of fungal DNA from lung homogenates.
591 E. Fungal burden determined by quantification of GMS staining.
592 F. Total number of CD45^{+} cells, eosinophils (CD45^{+}Ly6G^{-}CD11c^{-}SiglecF^{+}), AMs
593 (CD45^{+}Ly6G^{-}CD11c^{+}SiglecF^{+}), CD11c^{+}SiglecF^{-} (CD45^{+}Ly6G^{-} CD11c^{+}SiglecF^{-}), and CD11c^{-}SiglecF^{-}
594 (CD45^{+}Ly6G^{-}CD11c^{-}SiglecF^{-}) cells isolated from the mice with IA as determined by flow cytometry. *N*
595 = 4-6 mice per group.
596 G. qRT-PCR analysis for mRNA expression of the indicated cytokines.
597 H. TNFα secretion in BALF quantified by ELISA.

598 A-D, data are a summary of two to three independently performed experiments. F-H, data are
599 representative of two independent experiments with similar results. *$p < 0.05$, **$p < 0.01$, ***$p <$
600 0.001.

Figure 2.

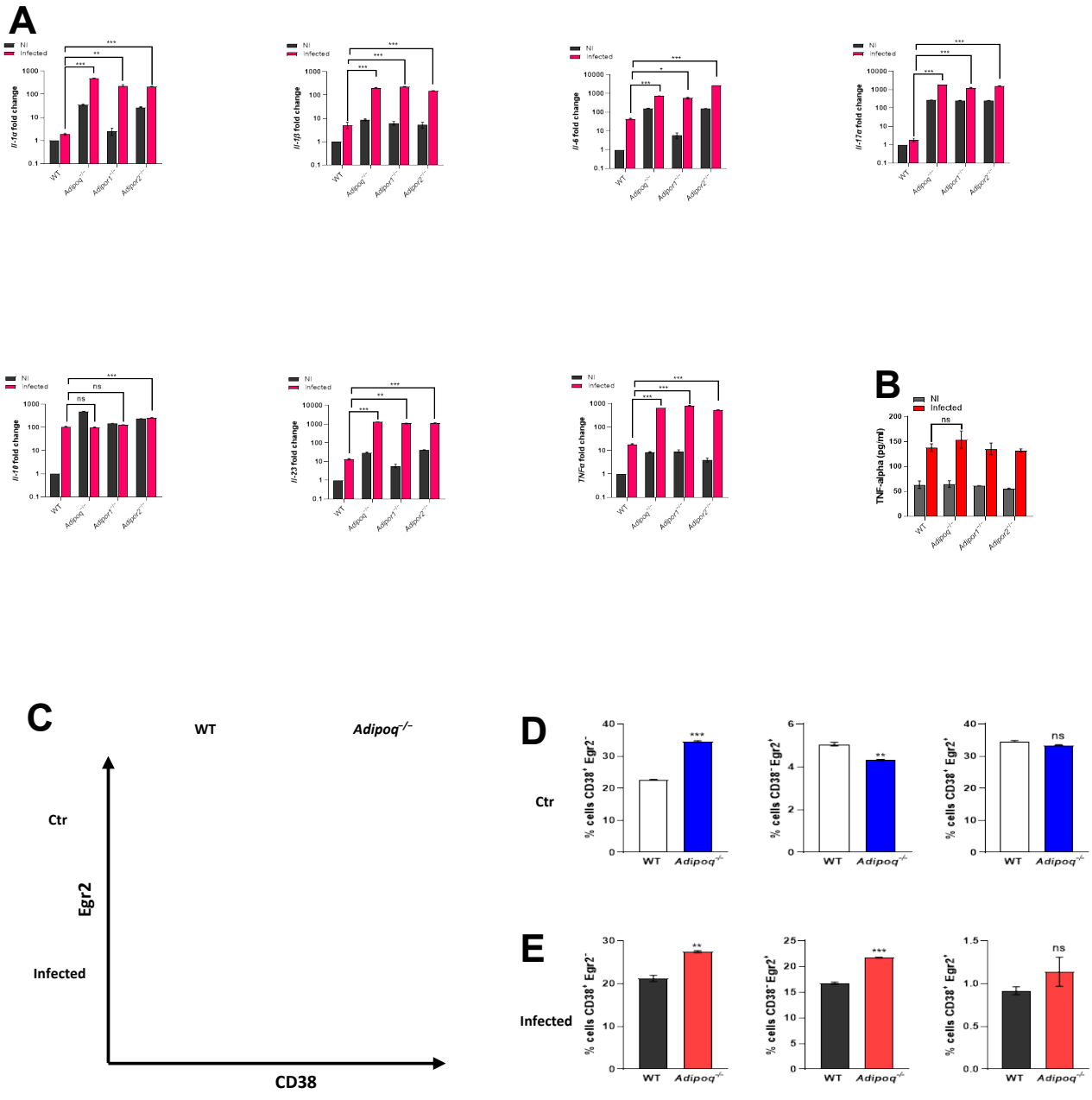
A
NI
Infected
Il-1α fold change
Il-1β fold change
Il-4 fold change
Il-17α fold change
Il-10 fold change
Il-23 fold change
TNFα fold change
WT
Adipoq-/-
Adipor1-/-
Adipor2-/-
B
TNF-alpha (pg/ml)
C
WT
Adipoq-/-
Ctr
Infected
Egr2
CD38
D
E
% cells CD38+ Egr2-
% cells CD38- Egr2+
% cells CD38+ Egr2+

602 **Figure 2. Alveolar macrophages from APN pathway-deficient mice exhibit an inflammatory**
603 **phenotype.**

604 BALF cells from wild-type (C57BL/6), APN-/- (*Adipoq*$^{-/-}$), *AdipoR1*$^{-/-}$, and *AdipoR2*$^{-/-}$mice were
605 collected in PBS/EDTA. For alveolar macrophage differentiation, total BALF cells were plated and
606 cultured with GM-CSF. Alveolar macrophages were challenged with conidia in the ratio 1:9 (AM :
607 conidia) for 10 hours duration as per the details mentioned in Materials and Methods. The data
608 represented is AMs from n=3 mice/group.

609 A. qRT-PCR analysis for mRNA expression of the indicated cytokines.
610 B. TNFα secretion quantified at the protein level by ELISA using *ex vivo* cultured alveolar
611 macrophages.
612 C. Flow cytometry staining of surface CD38 and intracellular Egr2

613 (D-E) Quantification of (C), showing the proportion of M1, M2 and CD38^{+}Egr2^{+} macrophages with
614 CD38^{+}Egr2^{-} (putative M1) or CD38^{-}Egr2^{+} (putative M2) phenotype in control group (D) and infection
615 group (E).

616 Data are a summary of three independently performed experiments. *$p < 0.05$, **$p < 0.01$, ***$p < 0.001$.

Figure 3.

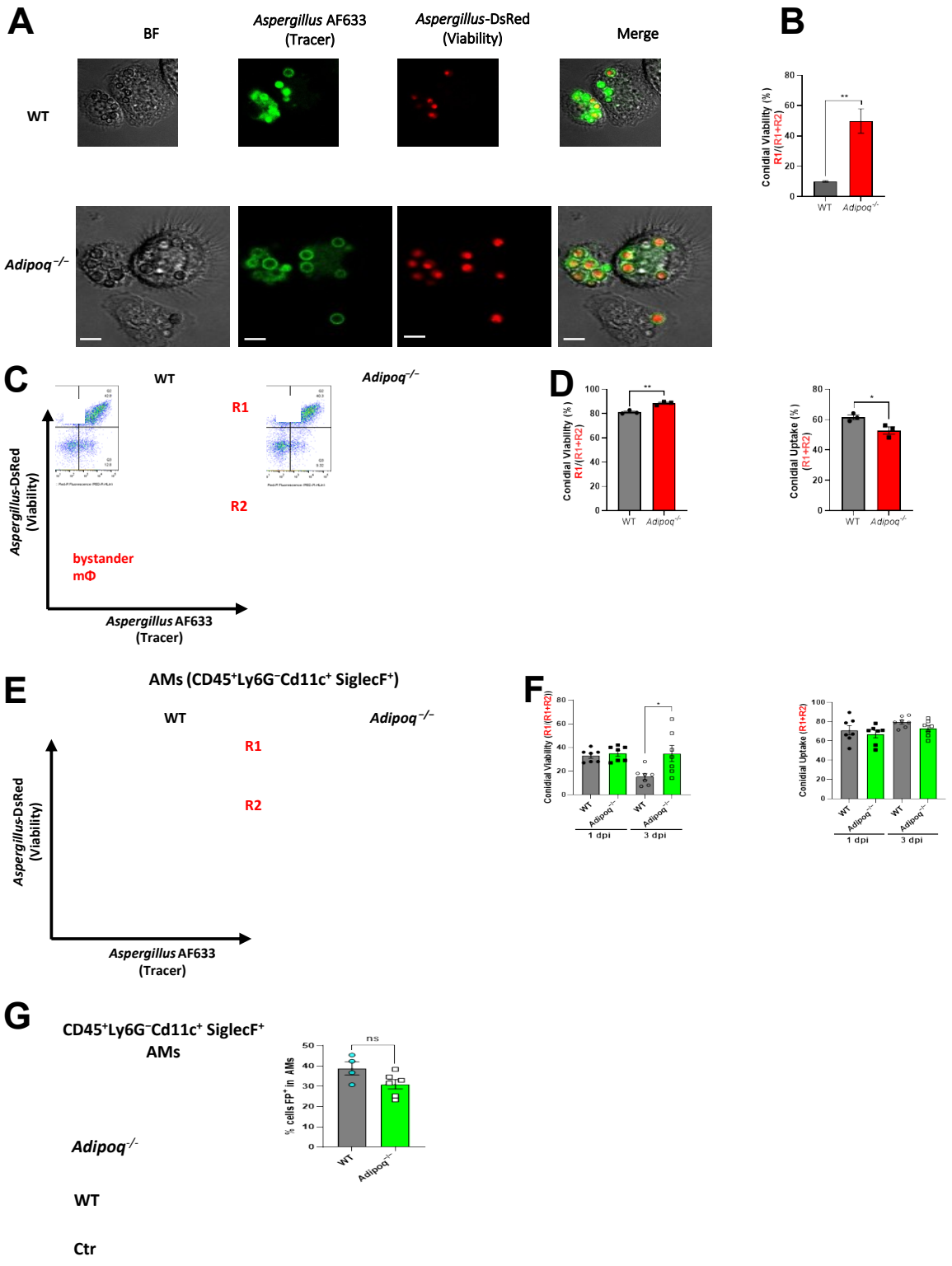
A
BF
Aspergillus AF633 (Tracer)
Aspergillus-DsRed (Viability)
Merge
WT
Adipoq-/-
B
Conidial Viability (%) R1/(R1+R2)
WT
Adipoq-/-
C
WT
Adipoq-/-
R1
R2
bystander mΦ
Aspergillus-DsRed (Viability)
Aspergillus AF633 (Tracer)
D
Conidial Viability (%) R1/(R1+R2)
Conidial Uptake (%) (R1+R2)
E
AMs (CD45+Ly6G-Cd11c+ SiglecF+)
WT
Adipoq-/-
R1
R2
Aspergillus-DsRed (Viability)
Aspergillus AF633 (Tracer)
F
Conidial Viability (R1/(R1+R2))
Conidial Uptake (R1+R2)
1 dpi
3 dpi
G
CD45+Ly6G-Cd11c+ SiglecF+ AMs
% cells FP+ in AMs
ns
Adipoq-/-
WT
Ctr

618 **Fig. 3. *A. fumigatus* conidial uptake and killing are inhibited in adiponectin-deficient AMs.**

619 A. Microscopic analysis of uptake and killing of FLARE conidia with magnification 40x is
620 depicted in Brightfield, Cy5, DsRed channels followed by the merged image. Scale bar is equal to
621 12µm.
622 B. Quantification of *Aspergillus* viability using microscopy images via calculation of co-
623 localization in imageJ.
624 C. Representative plots that display RFP and AF633 fluorescence intensity of *ex vivo* cultured
625 alveolar macrophages where R1 represents live conidia inside the alveolar macrophages and R2
626 represents dead/killed conidia .
627 D. Quantification of (C), showing *Aspergillus* viability (R1/(R1 + R2)) and uptake (R1 + R2) in *ex*
628 *vivo* cultured alveolar macrophages.
629 E. Representative plots that display RFP and AF633 fluorescence intensity of AMs
630 ($CD45^{+}Ly6G^{-}CD11c^{+}SiglecF^{+}$) *in vivo.* Mice of both groups were made immunocompromised and
631 infected with 1-1.5 × 10^{7} conidia. BAL cells were harvested 1 day and 3 days later.
632 F. Quantification of (E), showing *Aspergillus* viability (R1/(R1 + R2)) and uptake (R1 + R2) in
633 alveolar macrophages in neutropenic mice at d1 and d3 p.i.
634 G. Fluorescent particle uptake by alveolar macrophages in vivo. For flow cytometric analysis,
635 neutrophil-depleted mice were challenged with 1.5 × 10^{7} of flow particles. Percentage of flow particle
636 positive (FP+) cells was assessed in AMs ($CD45^{+}Ly6G^{-}CD11c^{+}SiglecF^{+}$) from the wild-type and *Adipoq*
637 $^{-/-}$ mice by flow cytometry.

638 A-D, data are representative of three independent experiments. E-G, data are a summary of 2-3
639 independent experiments. *$p < 0.05$, and **$p < 0.01$.

Figure 4.

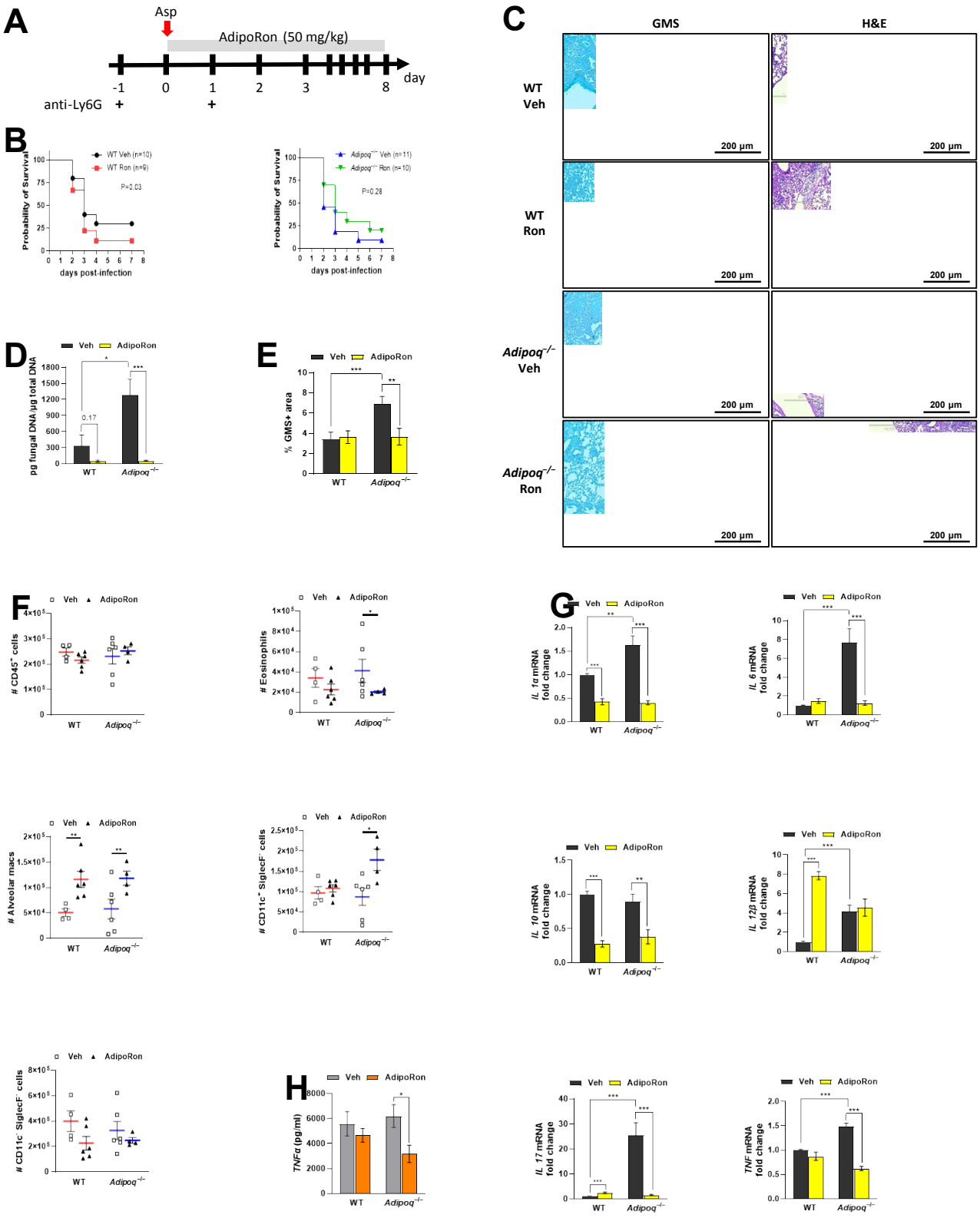
A
Asp
AdipoRon (50 mg/kg)
-1
0
1
2
3
8
day
anti-Ly6G
+
+
B
WT Veh (n=10)
WT Ron (n=9)
P=0.03
Probability of Survival
days post-infection
Adipoq-/- Veh (n=11)
Adipoq-/- Ron (n=10)
P=0.28
C
GMS
H&E
WT Veh
WT Ron
Adipoq-/- Veh
Adipoq-/- Ron
200 µm
D
Veh
AdipoRon
pg fungal DNA /µg total DNA
0.17
WT
Adipoq-/-
E
% GMS+ area
F
CD45+ cells
Eosinophils
Alveolar macs
CD11c+ SiglecF+ cells
CD11c- SiglecF- cells
G
IL 1α mRNA fold change
IL 6 mRNA fold change
IL 10 mRNA fold change
IL 12β mRNA fold change
IL 17 mRNA fold change
TNF mRNA fold change
H
TNFα (pg/ml)

641 **Figure 4. The AdipoR agonist AdipoRon improves decreases inflammation and fungal burden in**
642 **APN-deficient mice with IA**

643 Wild-type (C57BL/6), and *Adipoq*$^{-/-}$ mice were neutrophil depleted and involuntarily aspirated *A.*
644 *fumigatus* conidia as described in Materials and Methods.

645 A. Experimental time course for neutropenic mouse model of infection and AdipoRon treatment.
646 B. Effect of AdipoRon on the survival rate of WT and *Adipoq*$^{-/-}$ mice. N = 9-11 mice per group.
647 C. C. Representative GMS and H&E lung sections.
648 D. Fungal burden determined by quantitative PCR of fungal DNA from lung homogenates.
649 E. Fungal burden determined by quantification of GMS staining.
650 F. Total number of CD45^{+} cells, eosinophils (CD45^{+}Ly6G^{-}CD11c^{-}SiglecF^{+}), AMs
651 (CD45^{+}Ly6G^{-}CD11c^{+}SiglecF^{+}), CD11c^{+}SiglecF^{-} (CD45^{+}Ly6G^{-} CD11c^{+}SiglecF^{-}), and CD11c^{-}SiglecF^{-}
652 (CD45^{+}Ly6G^{-}CD11c^{-}SiglecF^{-}) cells isolated from the mice with IA as determined by flow cytometry. N
653 = 4-6 mice per group.
654 G. qRT-PCR analysis for mRNA expression of the indicated cytokines.
655 H. TNFα secretion in BALF quantified at the protein level by ELISA.

656 Data are a summary of 2-3 independently performed experiments. *$p < 0.05$, **$p < 0.01$, ***$p < 0.001$.

Figure 5.

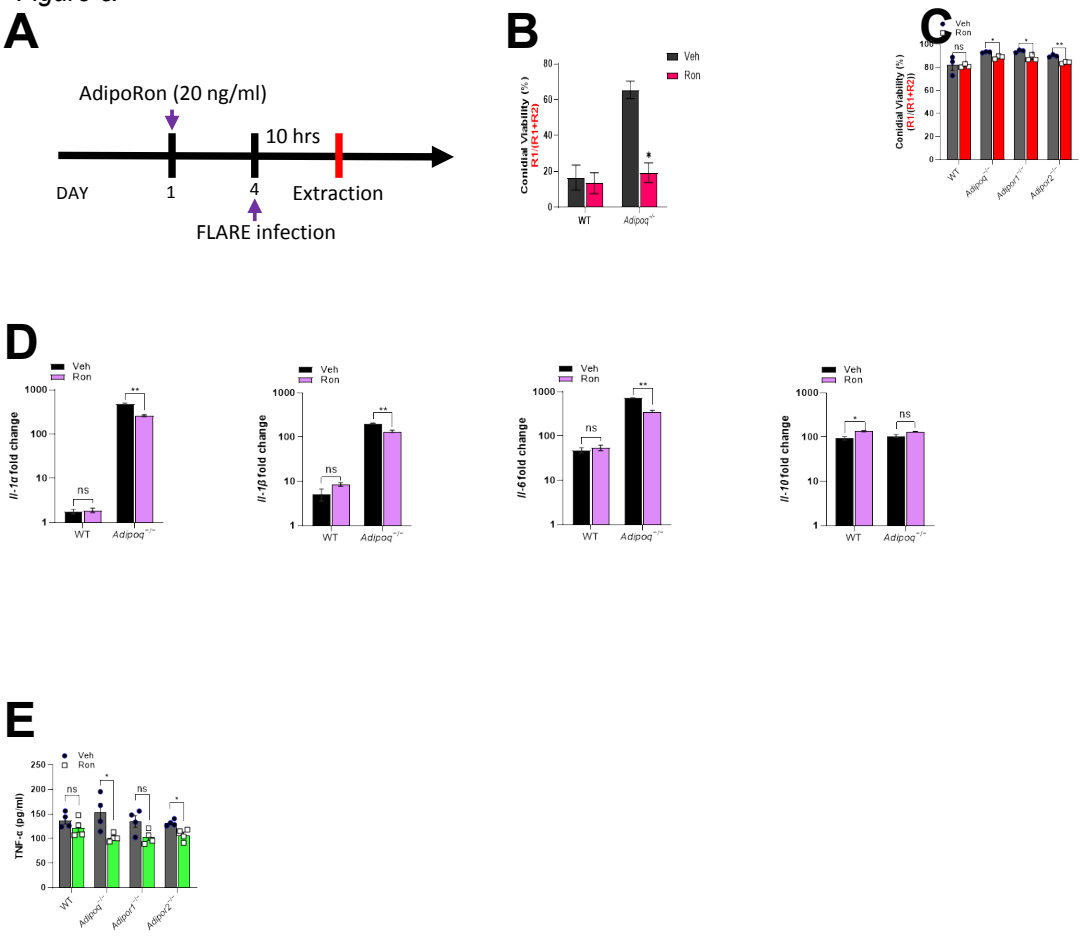
A
AdipoRon (20 ng/ml)
10 hrs
DAY
1
4
Extraction
FLARE infection
B
Veh
Ron
Conidial Viability (%)
R1/(R1+R2)
WT
Adipoq-/-
C
Veh
Ron
Conidial Viability (%)
(R1/(R1+R2))
WT
Adipoq-/-
Adipor1-/-
Adipor2-/-
D
Veh
Ron
Il-1α fold change
Il-1β fold change
Il-6 fold change
Il-10 fold change
WT
Adipoq-/-
E
Veh
Ron
TNF-α (pg/ml)
WT
Adipoq-/-
Adipor1-/-
Adipor2-/-

658 **Fig. 5. AdipoRon increases AdipoR-dependent AM fungal killing and reverses inflammatory**
659 **phenotype.**

660 A. Experimental time course for *ex vivo* cultured AMs challenged with conidia with or without
661 AdipoRon treatment.
662 B. Microscopic image quantification of *Aspergillus* viability (R1/(R1 + R2)) in *ex vivo* cultured
663 AMs by using FLARE conidia. The infection was done ex-vivo in 1:1 ratio (AMs: FLARE) for 15
664 hours.
665 C. Flow cytometric quantification of *Aspergillus* viability.
666 D. qRT-PCR analysis for mRNA expression of the indicated cytokines.
667 E. TNF secretion quantified at the protein level using *ex vivo* cultured AMs by ELISA.
668 Data are representative of three independently performed experiments. *$p < 0.05$, **$p < 0.01$, ***$p <$
669 0.001.

Figure 6.

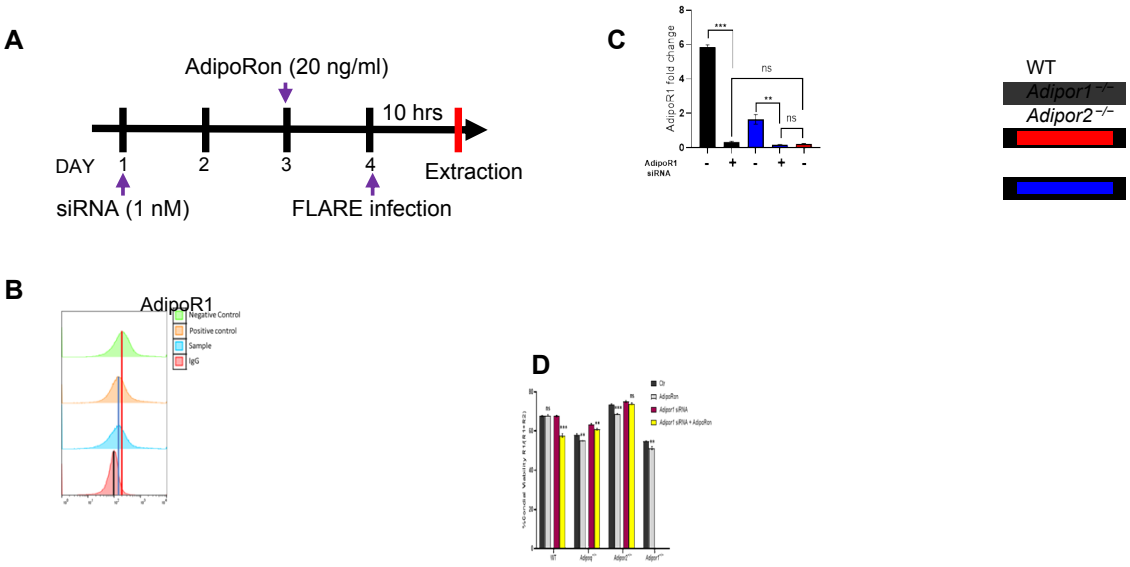
A
AdipoRon (20 ng/ml)
10 hrs
DAY
1
2
3
4
Extraction
siRNA (1 nM)
FLARE infection
B
AdipoR1
Negative Control
Positive control
Sample
IgG
C
AdipoR1 fold change
***
ns
**
ns
AdipoR1 siRNA
- + - + -
WT
Adipor1 −/−
Adipor2 −/−
D
Ctr
AdipoRon
Adipor1 siRNA
Adipor1 siRNA + AdipoRon

671 **Fig. 6. AdipoRon-enhanced killing of *A. fumigatus* requires both AdipoR1 and AdipoR2.**

672 A. Schematic timeline course for primary AM cultures treated with *AdipoR1* siRNA, details in
673 Methods section.
674 B. Histogram graphs obtained from flow cytometry analysis. The positive control represents the
675 ideal *Adipor1* knockdown control, while the negative control is in the absence of functional SiRNA.
676 C. qRT-PCR analysis for mRNA expression of the *adipor1* in AMs from the APN-deficient mice
677 with siRNA treatment.
678 D. Conidial viability (R1/(R1 + R2)) in *ex vivo* cultured AMs with siRNA and/or AdipoRon by
679 flow cytometry
680
681 Data are representative of two independently performed experiments. $^{**}p < 0.01$ and $^{***}p < 0.001$.

682

Figure 7.

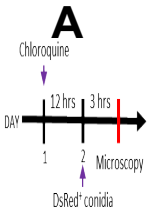
A
Chloroquine
12 hrs
3 hrs
DAY
1
2
Microscopy
DsRed+ conidia

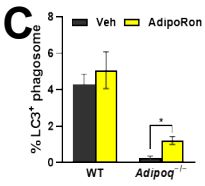
C
Veh
AdipoRon
% LC3+ phagosome
8
6
4
2
0
*
WT
Adipoq−/−

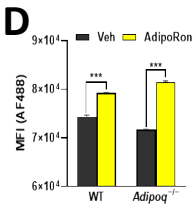
D
Veh
AdipoRon
MFI (AF488)
9×10⁴
8×10⁴
7×10⁴
6×10⁴
***
***
WT
Adipoq−/−

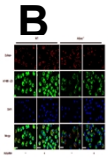
B

684 **Fig. 7. Adiponectin promotes LC3-associated phagocytosis of *A. fumigatus* conidia.**

685 A. Schematic timeline course for LC3-associated phagocytosis analysis.
686 B. Microscopy of LAP-dsRed conidia and $LC3^{+}$ AMs at a magnification of 20X in *ex vivo* cultured
687 AMs from infected WT and *Adipoq*$^{-/-}$ mice with or without AdipoRon. The images from DsRed, FITC,
688 DAPI channels are presented followed by the merged image. Scale bar: 35µm.
689 C. Microscopic quantification of $LC3^{+}$ phagosome (%) in *ex vivo* cultured AMs from infected WT
690 and *Adipoq*$^{-/-}$ mice with or without AdipoRon.
691 D. The mean fluorescent intensity (MFI) obtained by flow cytometry indicates the expression level
692 of LC3-AF488 in *ex vivo* cultured AMs from infected WT and *Adipoq*$^{-/-}$ mice with or without
693 AdipoRon.
694 Data are representative of two independently performed experiments. *$p < 0.05$ and ***$p < 0.001$.

695

696 **Supplemental Information**

697 **Supplemental Methods**

698 **Mice**

699 An additional strain of Adipoq-/- mice was obtained from Dr. Philipp Scherer (University of Texas-
700 Southwestern) and used for survival, fungal burden, histology, flow cytometric analysis of BALF cells,
701 qRT-PCR of selected inflammatory and *Adipor* genes, and ELISA for TNF as described in the
702 Materials and Methods section.

703 **Quantification of AM AdipoR1 expression using flow cytometry**

704 After ex-vivo AM extraction and culture as mentioned in the methods, AMs were fixed using IC
705 fixation buffer. Fc Block was used to eliminate non-specific Fc-mediated interactions. The cells were
706 then stained at a 1:100 dilution with primary antibody with Adiponectin Receptor 1 Recombinant
707 Rabbit Monoclonal Antibody (SC69-04) followed by staining with Alexa Fluor 488-conjugated goat
708 anti rabbit IgG as the secondary antibody. All the unstained and only primary antibody staining
709 controls were included.

710 **Quantification of AM *Adipor1* and *Adipor2* receptor gene expression**

711 RNA extraction from AMs was done using Qiagen RNeasy Mini kit, following the manufacturer's
712 protocol. Quantitative RT-PCR was performed with 20ng of cDNA using AdipoR1 and AdipoR2
713 forward and reverse primers ordered from IDT Integrated Technologies. Gene Expression Master Mix
714 (ThermoFisher Scientific) was used, with β-actin used for signal normalization.

715 **RNA sequencing and analysis**

716 **Sample Preparation**

717 AMs were isolated from APN-/- mice, infected/uninfected for 10 hours (1:9 cells/conidia) and
718 AdipoRon/vehicle treated 24 hours before infection, with cells lysed and RNA isolated as described in
719 Materials and Methods.

720 **Library preparation and sequencing**

721 Total RNA samples were first evaluated for their quantity and quality using Agilent TapeStation. All

722 the samples were good quality with RIN (RNA Integrity Number) of 9.6-10. One hundred nanograms
723 of total RNA was used for library preparation with the Illumina Stranded mRNA Prep, Ligation kit
724 (Illumina), following the manufacturer's instruction. Each resulting uniquely dual-indexed library was
725 quantified and quality accessed by Qubit and Agilent TapeStation, and multiple libraries were pooled
726 in equal molarity. The pooled libraries were sequenced with 2×150bp paired-end configuration on an
727 Illumina NovaSeq X PLUS sequencer.

728 **RNA-seq data analysis**

729 The sequencing reads were first quality checked using FastQC (v.0.11.5, Babraham Bioinformatics,
730 Cambridge, UK) for quality control. The sequence data were then mapped to the mouse reference
731 genome mm10 using the RNA-seq aligner STAR (v.2.7.10a)[52] with the following parameter: "--
732 outSAMmapqUnique 60". To evaluate quality of the RNA-seq data, the number of reads that fell into
733 different annotated regions (exonic, intronic, splicing junction, intergenic, promoter, UTR, etc.) of the
734 reference genome was assessed using bamutils (from ngsutils v.0.4.17).[53] Uniquely mapped reads
735 were used to quantify the gene level expression employing featureCounts (subread v.2.0.3)[54] with the
736 following parameters: "-s 2 -Q 10". The data was normalized using TMM (trimmed mean of M values)
737 method. Differential expression analysis was performed using edgeR (v.4.0.1).[54,55] False discovery
738 rate (FDR) was computed from p-values using the Benjamini-Hochberg procedure. Gene Ontology
739 (GO) pathway enrichment analyses were performed with the R package clusterProfiler.[56,57]

Supplemental Figure S1.

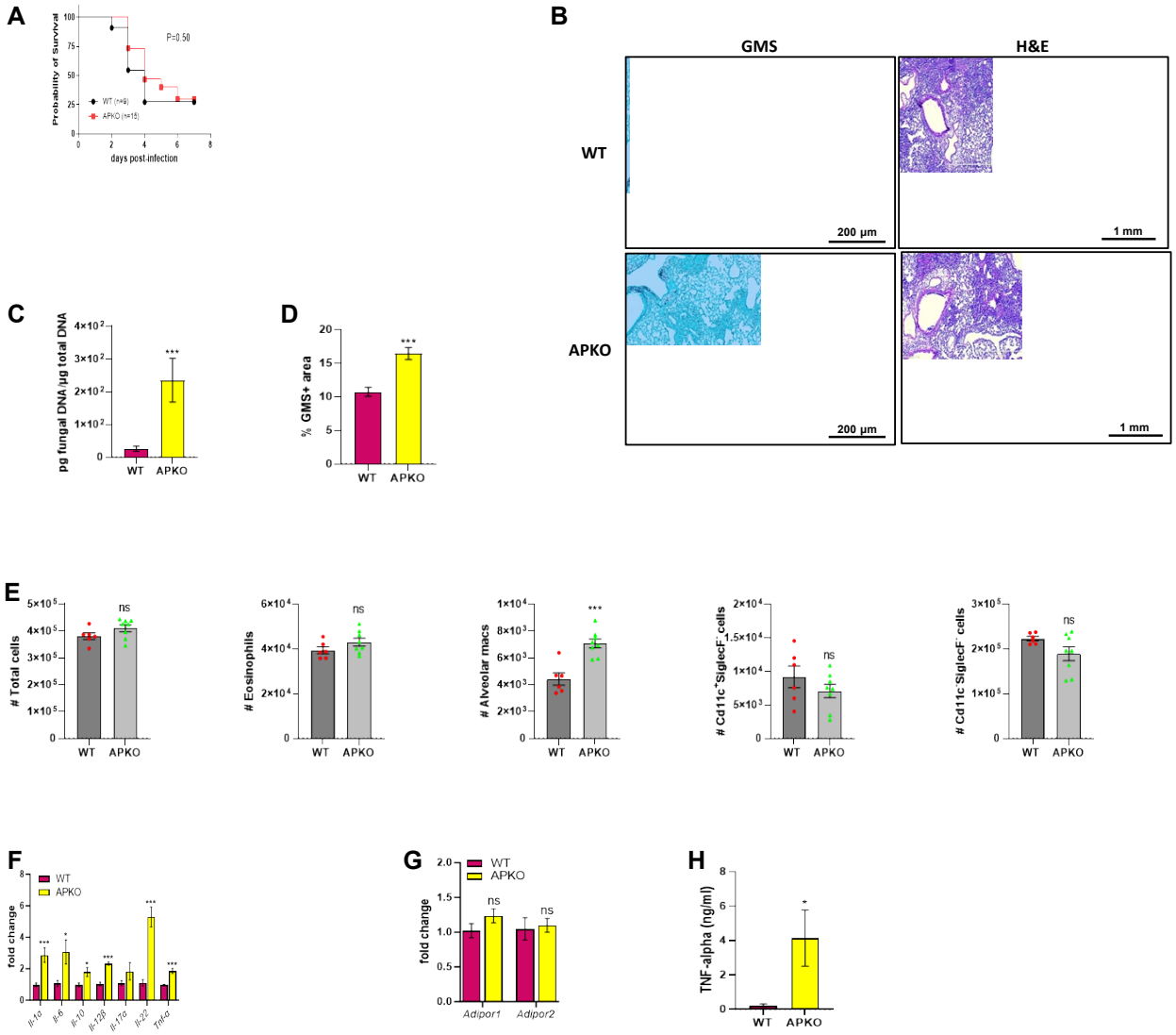

741 **Fig. S1. Inflammatory phenotype of APN-/- mice from a second strain.**

742 Wild-type (C57BL/6) and APKO (Second *Adipoq*$^{-/-}$ mice from Scherer's laboratory) were neutrophil
743 depleted and involuntarily aspirated 1 – 1.5 × 10^7 of conidia as described in Materials and Methods.

744 A. Survival rate. N = 9 and 15 mice per group, respectively.
745 B. Representative GMS and H&E lung sections.
746 C. Fungal burden determined by quantitative PCR of fungal DNA from lung homogenates.
747 D. Fungal burden determined by quantification of GMS staining.
748 E. Total number of CD45$^+$ cells, eosinophils (CD45$^+$Ly6G$^-$CD11c$^-$SiglecF$^+$), AMs
749 (CD45$^+$Ly6G$^-$CD11c$^+$SiglecF$^+$), CD11c$^+$SiglecF$^-$ (CD45$^+$Ly6G$^-$ CD11c$^+$SiglecF$^-$), and CD11c$^-$SiglecF$^-$
750 (CD45$^+$Ly6G$^-$CD11c$^-$SiglecF$^-$) cells isolated from the mice with IA as determined by flow cytometry. N
751 = 4-6 mice per group.
752 F. qRT-PCR analysis for mRNA expression of the indicated cytokines.
753 G. qRT-PCR analysis for mRNA expression of *Adipor1* and *Adipor2*.
754 H. TNFα secretion in BALF quantified at the protein level by ELISA.

755 Data are a summary of two to three independently performed experiments. *$p < 0.05$, **$p < 0.01$, ***p
756 < 0.001.

757

Supplemental Figure S2.

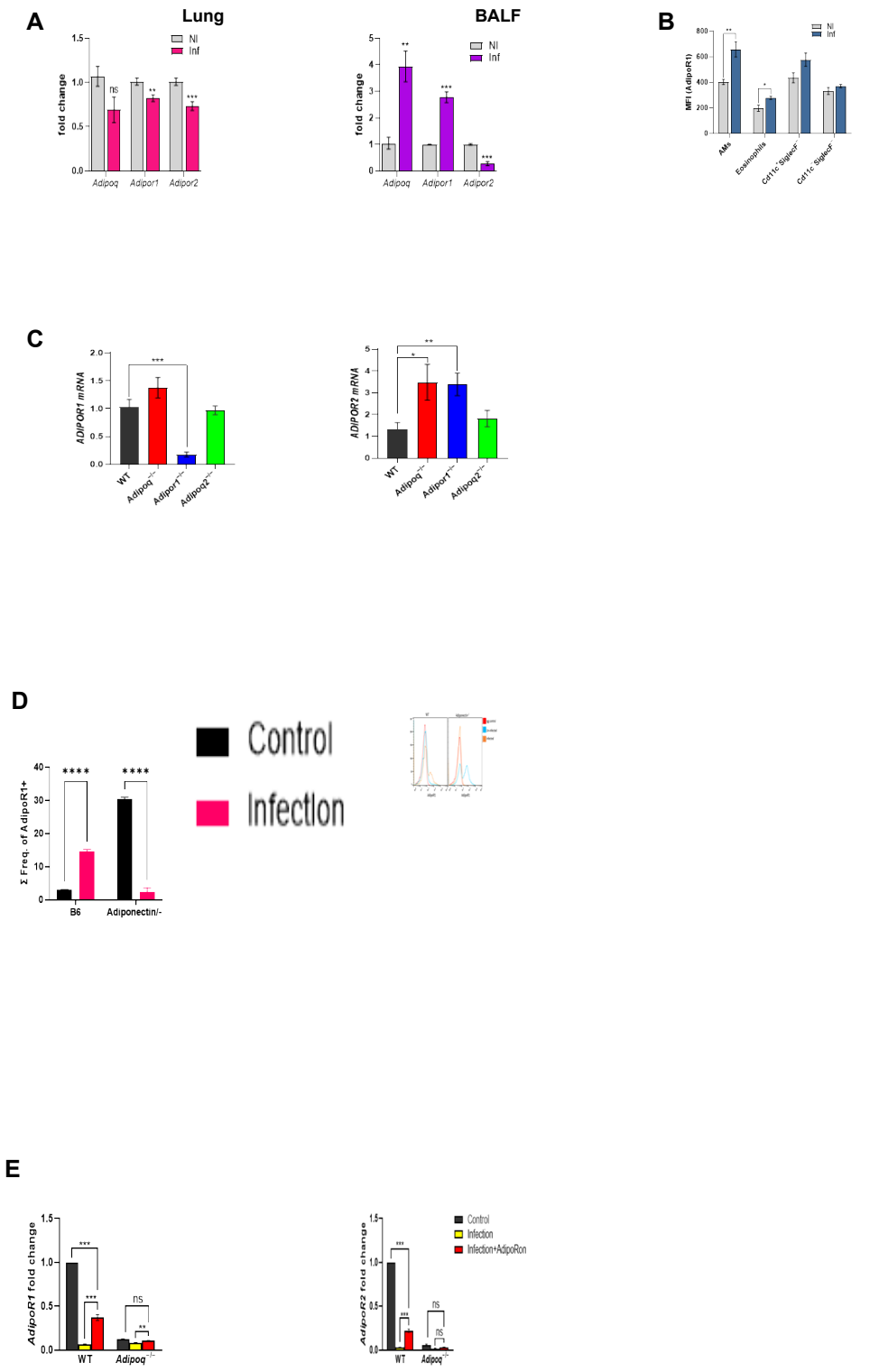

759 **Fig. S2. AdipoRs expression in the Lung and BALF in APN pathway-deficient mice with invasive**
760 **aspergillosis.**

761

762 A. Expression of *Adipoq* and *Adipor* genes in lung homogenates and BALF cells from non-
763 infected (NI) and conidia-infected WT mice. Lung and BALF were collected from the mice at 3 dpi.
764 B. Summary of median fluorescence intensities of AdipoR1 staining on AMs
765 ($CD45^{+}Ly6G^{-}CD11c^{+}SiglecF^{+}$), eosinophils ($CD45^{+}Ly6G^{-}CD11c^{-}SiglecF^{+}$), $CD11c^{+}SiglecF^{-}$
766 ($CD45^{+}Ly6G^{-}$ $CD11c^{+}SiglecF^{-}$), and $CD11c^{-}SiglecF^{-}$ ($CD45^{+}Ly6G^{-}CD11c^{-}SiglecF^{-}$) cells from non-
767 infected (NI) and conidia-infected WT mice.
768 C. qRT-PCR analysis for mRNA expression of *Adipor1* and *Adipor2* in lung homogenates. Wild-
769 type (C57BL/6), *Adipoq*$^{-/-}$, *AdipoR1*$^{-/-}$, and *AdipoR2*$^{-/-}$mice were neutrophil depleted and involuntarily
770 aspirated *A. fumigatus* conidia.
771 D. Flow cytometry staining of AdipoR1. Frequency of AdipoR1+ in ex-vivo cultured AMs in WT
772 and *Adipoq*$^{-/-}$ mice. The histogram represents the AdipoR1 peak relative to IgG control in infected vs
773 uninfected.
774 E. qRT-PCR analysis for mRNA expression of *Adipor1* and *Adipor2* from the ex-vivo cultured
775 AMs. The AMs were challenged with AF-293 conidia with or without AdipoRon treatment.

776 Data are a summary of two to three independently performed experiments. *$p < 0.05$, **$p < 0.01$, ***p
777 < 0.001.

778

Supplemental Figure S3.

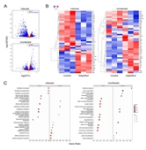

780 **Fig. S3 Gene expression in AdipoRon treated/untreated and infected/ uninfected *Adipoq*$^{-/-}$ AMs**
781 **by RNAseq analysis.**

782 AMs were infected with swollen AF293 conidia with 1:9 cells/conidia for 10 hours, or left uninfected,
783 with or without AdipoRon treatment, followed by RNA extraction for RNAseq analysis (N=3/group).

784 A. Volcano plot depicting relative changes in gene expression of AdipoRon-treatment in APN-/-
785 AMS, infected (top) or uninfected (bottom).
786 B. Heat map representation of the genes with highest differential expression in infected (left) and
787 uninfected (right) APN-/- AMs.
788 C. GSEA-GO analysis of gene pathways that are both differentially expressed by AdipoRon treatment
789 in infected (left) and uninfected (right) APN-/- AMs.
790

791 **Supplemental Video SV1. Time course of uptake and killing in WT and APN-/- AMs.**

792 Alveolar macrophages were plated and infected as mentioned in the methods. Cells were live imaged
793 by confocal microscopy for T= 8min under 40X water immersion lens. The black arrows indicate the
794 live conidia at T=0 min and the white arrows indicate the conidia at T=8min.

795

796